



Wearable sensors for automatic detection of trauma procedures

Master's Thesis of

David Greiner

at the Department of Informatics
Institute for Anthropomatics and Robotics

Reviewer: Prof. Dr. U. Hanebeck
Second reviewer: Prof.
Advisor: Prof. Dr. Julie A. Adams
Second advisor: M.Sc. Jamison Heard

January 14th, 2018 – July 14th, 2018

Karlsruher Institut für Technologie
Fakultät für Informatik
Postfach 6980
76128 Karlsruhe

I declare that I have developed and written the enclosed thesis completely by myself, and have not used sources or means without declaration in the text.

PLACE, DATE

.....

(David Greiner)

Abstract

Accurate information is vital when transferring patients care between emergency medical services and the hospital trauma team. This thesis proposes an automatic procedure detection system using accelerometer, gyroscope, and electromyography data to recognize a subset of common procedures performed on trauma patients. The following five procedures were chosen for this thesis: cardiopulmonary resuscitation, bag-valve-mask ventilation, placing an oral airway, placing an intravenous tourniquet, and wrapping a head wound. The procedures were then decomposed into their anatomical movements using hierarchical task analysis. The resulting anatomical movements were analyzed to include their sensability using five commercially available sensors: Apple Watch, Myo, Empatic E4, Garmin Watch Forerunner, and Biopac Bioharness BT. The Myo wearable device was chosen for its capability to sense the majority of the anatomical movements. Three machine learning algorithms: decision-tree, SVM, and k -NN were trained and compared to a Hidden Markov Model. The features included: mean, standard-deviation, signal magnitude area, root mean squared, and power spectral density. The decision-tree received the highest F1-score of 0.73, followed by HMM with 0.44, k -NN ($k = 1$) with 0.44, and SVM with 0.33.

Zusammenfassung

Genaue Informationen sind wichtig, wenn die Verantwortung für Patienten von Rettungssanitätern im Krankenwagen an Krankenhauspersonal übertragen wird. Diese Masterarbeit schlägt ein automatisches Behandlungserkennungs-System vor, welches durch Beschleunigungs-, Orientierungs- und Muskeldaten einen Teil von üblichen Behandlungen an Traumapatienten erkennt. Für diese Arbeit wurden die folgenden fünf Verfahren ausgewählt: kardiopulmonale Reanimation, Masken-Beatmung, Einführung eines oralen Luftweges, Platzierung eines Venenstauer und Bandagieren einer Kopfwunde. Die Verfahren wurden unter Verwendung einer hierarchischen Aufgabenanalyse in ihre anatomischen Bewegungen zerlegt. Fünf handelsübliche Sensoren: Apple Watch, Myo, Empatic E4, Garmin Watch Forerunner und Biopac Bioharness BT wurden dahingehend analysiert, wie genau die anatomischen Bewegungen erkannt werden können. Das am Unterarm tragbare Myo-Gerät wurde aufgrund seiner Fähigkeit ausgewählt, die meisten anatomischen Bewegungen zu erfassen. Drei maschinelle Lernalgorithmen: Entscheidungsbaum, SVM und k -NN wurden trainiert und mit einem Hidden-Markov-Modell verglichen. Die Features umfassten: Mittelwert, Standardabweichung, Signalbetragbereich, quadratischer Mittelwert und spektrale Leistungsdichte. Der Entscheidungsbaum erreichte den höchsten F1-Wert von 0.73, gefolgt von HMM mit 0.44, k -NN ($k = 1$) mit 0.44 und SVM mit 0.33.

Contents

Abstract	i
Zusammenfassung	iii
1. Problem Statement	1
2. Literature Review	3
2.1. Hand-Off Communication	3
2.2. Human Activity Recognition	4
2.2.1. External Sensors	5
2.2.2. Wearable Sensors	6
2.2.3. Differences	7
2.3. Machine Learning within Human Activity Recognition	8
2.3.1. Coarse-grained movements	9
2.3.2. Fine-grained movements	10
2.3.3. Intention Recognition	11
2.3.4. Discussion	12
2.4. Summary	13
3. Methodology	15
3.1. Hierarchical Task Analysis	15
3.2. Algorithm	18
3.2.1. Data Acquisition	18
3.2.2. Data Processing	18
3.2.3. Feature Extraction	19
3.2.4. Machine Learning	21
3.3. Experimental Design	23
3.3.1. Data Collection	23
3.3.2. Participant Demographics	24
3.3.3. Machine Learning	24
3.3.4. Research Questions	24
4. Results	25
4.1. IMU and EMG Patterns	26
4.1.1. IMU and EMG Patterns Discussion	31
4.2. Individual Participant Results	32
4.2.1. Individual Participant Results Discussion	33

4.3. Participant Generalizability	34
4.3.1. Participant Generalizability Discussion	35
4.4. Discussion	36
5. Conclusion	39
Bibliography	41
A. Appendix	49
A.1. Machine Learning Algorithms Parameters	55
A.2. 2 Seconds and 4 Seconds Window Sizes	56

List of Figures

3.1. EMS procedures	15
3.2. Myo Reference Frame (Source: http://developerblog.myo.com/gui-without-g-going-beyond-screen-myotm-armband/)	18
3.3. Myo Gestures (Source: https://dribbble.com/shots/1937560-Gesture-Icons)	18
3.4. HMM state diagram for EMS procedures	22
4.1. IMU Data Plots for Acceleration and Orientation Data for CPR	26
4.2. EMG Data Plots for CPR	27
4.3. EMG Data Plots for Bag-Valve-Mask ventilation	27
4.4. IMU Data Plots for Acceleration and Orientation Data for Bag-Valve-Mask ventilation	28
4.5. IMU Data Plots for Acceleration and Orientation Data for Placing an Oral Airway	29
4.6. EMG Data Plots for Placing an Oral Airway	29
4.7. IMU Data Plots for Acceleration and Orientation Data for Placing an IV Tourniquet	30
4.8. EMG Data Plots for Placing an IV Tourniquet	30
4.9. IMU Data Plots for Acceleration and Orientation Data for wrapping a head wound	31
4.10. EMG Data Plots for Wrapping a Head Wound	31
4.11. Tourniquet EMG data with average in red	35

List of Tables

2.1.	Summary of Human Activity Recognition sensors	5
2.2.	Summary of the Reviewed Machine Learning Algorithms	9
3.1.	Hierarchical Task Analysis: Overview	16
3.2.	Features for the Machine Learning algorithm	19
4.1.	Ten-fold cross validation for detecting CPR per participant. Note: Bold represents the highest performance across a row	33
4.2.	Ten-fold cross validation for detecting BVM ventilation per participant .	34
4.3.	Ten-fold cross validation for detecting oral airway placement per participant	35
4.4.	Ten-fold cross validation for detecting tourniquet placement per participant	36
4.5.	Ten-fold cross validation for detecting wrapping a wound per participant	37
4.6.	Ten-fold cross validation for all participants by procedure and algorithm. Note: T is intravenous tourniquet, W is wrapping a wound, B is Bag-Valve-Mask ventilation, O is oral airway, and C is CPR	37
A.1.	Hierarchical Task Analysis: CPR	50
A.2.	Hierarchical Task Analysis: Bag-Valve-Mask Ventilation	51
A.3.	Hierarchical Task Analysis: Placing an Oral Airway	52
A.4.	Hierarchical Task Analysis: Placing an IV Tourniquet	53
A.5.	Hierarchical Task Analysis: Wrapping a wound	54
A.6.	2 seconds. Note: T is intravenous tourniquet, W is wrapping a wound, B is Bag-Valve-Mask ventilation, O is oral airway, and C is CPR	56
A.7.	4 seconds	56

Glossary

CPR Cardiopulmonary Resuscitation.

EMG Electromyography.

EMS Emergency Medical Services.

HAR Human Activity Recognition.

RMS Root Mean Square.

SMA Signal Magnitude Area.

1. Problem Statement

Treating a person with severe trauma is extremely challenging, as the injury may result in life-threatening effects on blood circulation and tissue oxygenation. Every decision can make the difference between life and death. After the first assessment by the emergency medical services (EMS), the patient's medical state has to be monitored continuously. Upon arrival at the hospital, it is important for the trauma team to understand the patient's treatment history, including what medications have been administered and emergency procedures have been performed. This information is vital to providing the most accurate and beneficial care; however, such life-critical information may not be properly communicated when transferring the patient from the EMS personnel's care to the hospital trauma team. EMS personnel often rely on their memory to communicate the patient's treatment history, which can be inaccurate. Failing to communicate a complete and accurate treatment history can lead to permanent damage or death. This thesis proposes an automatic reporting system using accelerometer, gyroscope, and electromyography (EMG) data to detect a subset of common procedures performed on trauma patients. An algorithm that incorporates machine learning will be developed to classify the subset of EMS procedures based on the wearable sensor data.

Automatically detecting trauma procedures may improve the communication during the care transfer between EMS personnel and the trauma team. Some ambulances are equipped with devices that record the patient's vitals and statistics about cardiopulmonary resuscitation (CPR), such as the duration, frequency, and depth of the chest compressions. Missing from these devices is the ability to automatically detect other common EMS procedures. Information about the patient's care is typically entered into the patient's transcript after completing the patient hand-off to the trauma team. When arriving at the hospital, paramedics can provide records e.g., graphs and vital statistics, on a tablet, in addition to the standard oral communication protocol. The full transcript is transmitted via the Internet to the hospital's database when connected to the secured city network. The data transfer usually does not occur until the ambulance arrives back at the station. Currently, transferring patient care information is a slow and static process. Real-time information about the patient's state will be beneficial for the trauma team before the patient arrives at the hospital, as this advanced information knowledge allows the hospital staff to properly prepare the emergency room for the severity of the case.

The proposed detection of a subset of commonly performed EMS procedures on trauma patients includes CPR, airway management, placing an intravenous tourniquet, and wrapping a wound. CPR is the process of helping a person breath using chest compressions and artificial ventilation. Airway management consists of multiple procedures depending on the severity of the trauma. Bag-valve-mask ventilation provides air for patients with breathing difficulties, while an oropharyngeal device is used to manage an unresponsive patient's airway. Oropharyngeal devices keep the tongue from obstructing the airway.

1. Problem Statement

Some trauma patients require intubation, in which a tube is inserted orally and reaches into the windpipe. Intravenous tourniquet are tied on a patient's arm to highlight veins. Wrapping a wound is a procedure to stop the bleeding from an open wound and prevent infection.

The EMS procedures were decomposed into their anatomical movements using hierarchical task analysis, which determined that each EMS procedure requires a specific sequence of anatomical movements. Each sequence generates patterns in the accelerometer, gyroscope, and EMG data, which the developed task recognition algorithm will detect.

A major challenge of detecting a procedure is that the EMS personnel must use two arms to perform the necessary care for the patient. Therefore, each arm must be monitored and both datasets have to be integrated and analyzed by the automatic task recognition algorithm. A second challenge is that there are individual differences in the body movements when executing EMS procedures. Depending on the EMS personnel, body movements vary from using a different finger to another motion. Another challenge is accounting for an ambulance's abrupt turns, fast acceleration, and sudden stops, as such ambulance movements generate noise on the accelerometer and gyroscope data unrelated to the EMS personnel's movement and must be filtered.

Chapter 2 provides background information on existing systems to detect physical movement. Chapter 3 lays out the criteria for the algorithm and hypothesis for the outcome of a user study, and provides an algorithm that detects trauma procedures by EMS personnel. Additionally an experimental design for studies to collect data and test the algorithm is introduced. Chapter 4 presents the results of the studies. Finally, Chapter 5 outlines the contribution and drawbacks of the algorithm, followed by a discussion how future work can improve the system.

2. Literature Review

2.1. Hand-Off Communication

A hand-off in the medical community is the process of transferring a patient from one care provider to another [62]. During the hand-off process key information is communicated, e.g., the patient's state, administered medication, and treatment. The emergency medical service (EMS) hand-off process consists of multiple stages. Initially, patient information is communicated to the hospital trauma team during patient transport. Once the patient arrives, and care is transferred from the EMS personnel to the hospital, more detailed information is communicated. Compared to the initial information, the detailed information includes personal data, such as address, insurance information, previous injuries, etc. and a step-by-step list of treatment events. Finally, after the EMS return to the rescue station, a complete report of the patient's treatment is compiled, and the process is complete [17].

Inadequate communication is the leading cause of malpractice lawsuits; in 2015, three out of ten malpractice lawsuits mention a breakdown in communication [20]. Doctors spend most of their time communicating with patients and other care providers. An observation of doctors for 35 hours and 13 minutes found that doctors engaged in communication events 78.7% of the time [63]. When a patient arrives at the hospital, communication between hospital staff can take place in several different ways. Bhabra, Mackeith, Monteiro, and Pothier [9] compared information loss during hand-off for three communication methods: verbal communication, verbal communication with note-taking, and exchange of a printed treatment record by the person handing off the patient to the person assuming the responsibility of care. Every participant received the same communication in every cycle. After five cycles the information loss when communicating verbally was 97.5%, note-taking by the receiving person incurred a 14.5% information loss, and handing a printed sheet to the receiving person resulted in 1.25% information loss [9]. The small information loss during communication using a printed sheet was due to the amount of information a participant had to remember. The only information loss when exchanging a printed sheet occurred during the fifth cycle, while 100% of the information was retained during all previous cycles. Bhabra et al.'s study focused on in-hospital care transfer and did not consider time critical or trauma situations. A study of hand-offs between EMS personnel and emergency department staff found that the quality of information exchange in the emergency department is higher for trauma patients than for non-trauma patients [50]. EMS personnel reported that when handling trauma cases, the emergency department staff were highly engaged and desired a detailed report, while emergency department staff were less interested in non-trauma patients.

The Joint Commission on Accreditation of Healthcare Organizations set a goal to improve medical hand-off communication [5]. The commission conducted a study and

2. Literature Review

found that the hand-off communication process is highly variable and discipline-specific. Therefore, every discipline and department developed a protocol specific to their unique requirements. A study comparing medical errors and preventable adverse events before and after the introduction of a standardized hand-off communication protocol for patient admission at nine pediatric residency training programs in the United States and Canada was conducted. The study found that the medical error rate during the EMS hand-off process decreased by 23%, and the rate of preventable adverse events decreased by 30% after the implementation of a standardized hand-off communication protocol [64]. An automatic detection system can provide additional information that an EMS personnel may have missed, further increasing the reporting accuracy and decreasing the medical error rate.

Hand-off communication in nursing is commonly done using an Electronic Health Record. Electronic Health Records store a patient's medical records and allow medical professionals to input vital data and share treatment information. It was determined, that using these systems improved the continuity of care and increased the consistency of data [18]. The existing Electronic Health Record can be updated using an automatic detection system to provide real-time information regarding a patient's care, from the time the EMS personnel arrive at the scene until the hand-off at the hospital.

The hand-off communication between EMS personnel and the hospital's team presents unique challenges. Both sets of personnel have different worksites and clinical duties, which may result in communication errors due to the personnel being unfamiliar with each others' procedures. The time window during which the communication occurs is extremely short. Information communication during transport is limited due to the urgency to provide care to the patient. Automatically detecting procedures may augment the verbally communicated information and may be sent in real-time through a different communication modality. Depending on the patient's level of acuity, emergency department staff may pay less attention during the hand-off communication, if the injuries are deemed non-life-threatening [62, 50]. If a patient with a common injury arrives, emergency department staff may assume they already know everything about the case; therefore, potentially missing critical information and resulting in permanent injury or death.

2.2. Human Activity Recognition

Human Activity Recognition (HAR) is a method intended to recognize common human activities in real life settings [30]. HAR uses patterns discovered from low-level sensor data to train activity models that can be used to detect the human's activity.

Increasing interest in HAR has lead to improved computational power, smaller size, and lower cost of sensors [58]. The sensors used to recognize human activities fall into two categories: *external* and *wearable* sensors [43]. An external sensor observes the human from a fixed point of view and relies on human interaction within the sensor's range and field of view. A wearable sensor is worn on the user's body and collects information as the human conducts their activities. The reviewed sensor types and the anticipated associated advantages and disadvantages for automatically detecting EMS procedures are provided

Table 2.1.: Summary of Human Activity Recognition sensors

Sensor	Advantages	Disadvantages
Camera	Captures all body parts of the human Not worn on the body Higher information flow Capture information around the human	Requires human to be in field of view Higher privacy invasion Computational expensive Requires good lighting
Environmental	Senses the environmental context of the human	Not very accurate for HAR
Acceleration	Most accurate wearable sensor for HAR	Sensor placement can make a difference
Location	Useful for detecting transportation	Not useful for fine-grained detection
Physiological	Useful for measuring human's activity load	Activity load is different depending on fitness level

in Table 2.1. The following chapter examines the advantages and disadvantages for each sensor and how they can be used to automatically detect EMS procedures.

2.2.1. External Sensors

Extensive HAR research has focused on using cameras as external sensors to visually recognize gestures and movement. Visual recognition has two primary sources of data: RGB and grayscale video. RGB data is the visual representation of the camera in pixels of red, green, and blue values. Grayscale data is the depth representation of the camera in a shade of gray, white being closest and black being the furthest away. Multiple features can be extrapolated from the video data, e.g., body part detection [13], motion detection [1]. A common analysis approach uses background subtraction to project a silhouette onto a person, which allows for the detection of a region of interest within which motion occurs [11]. Isolating this motion permits a more detailed analysis of the region of interest. Motion around the patient, in the context of an ambulance, indicates that a procedure is likely being performed. Using multiple cameras, it is possible to generate 3D models with silhouettes of humans [70]. 3D models are used to generate information regarding the positioning of human limbs, the human's distance relative to other objects, and the human's pose.

Regions of interest can be detected using motion information in the video. The difference between video frames is analyzed pixel-wise to determine the direction of the movement, making it useful for detecting moving objects when the camera is steady [23]. Humans are rarely stationary; therefore the motion information can be used to generate features, such as the human's speed.

2. Literature Review

Joint angle detection is more complex than detecting silhouettes. Joint detection provides a richer dataset to a HAR algorithm, which can increase the algorithm's accuracy [25]. Joint detection requires a 3D scene to maintain a representation that is view-invariant [56]. Using joints and their angles allows for reconstructing and identifying the human skeleton. Understanding the human skeletal position allows for more accurate classifications of skeletal-based human activities, such as waving an arm, jumping, or sitting [15].

2.2.2. Wearable Sensors

Wearable sensors come in all shapes and sizes. Most people never notice how many sensors are carried around in their devices on a daily basis. Wearable sensors for human activity recognition fall into one of four groups: environmental attributes, acceleration, location, and physiological signals [43]. Sensors for environmental attributes do not collect data about the human, but rather about the human's surrounding environment [55]. A sensor for environmental attributes is the air pressure sensor which measures the altitude of the human [10], or the humidity sensor which measures the amount of water vapor in the air [40]. An acceleration sensor senses the movement of the body part on which it is placed, relative to the whole body movement [49]. Acceleration sensors may contain up to three axes (X,Y,Z). A popular use for acceleration sensors in smartphones is step counting of the human's activity [12]. Location sensors determine the location of the human as coordinates on a map [57]. For example, a Global Positioning System (GPS) sensor uses satellites in space to triangulate a human's position to latitude, longitude, and elevation [32]. Physiological signals sensors monitor the human's vital signs [72]. For example, heart rate, respiration rate, skin temperature, and electrocardiogram amplitude can be used to improve activity recognition [44].

Environmental attributes relate to the human's surroundings, e.g., temperature, noise level, and light intensity [49]. These environmental attributes allow for detecting the climate the human is currently experiencing. For example, using the air pressure an approximate location of the human in a subway system can be determined [24]. Depending on the environmental attributes, humans may be more likely to take part in certain activities, such as walking in sunshine and warm weather. Environmental attribute information may be insufficient as the sole means of recognizing human activity.

The most broadly used HAR sensors are the accelerometer and gyroscope sensors [43]. The acceleration and gyroscope sensors are commonly found in almost every smart device, e.g., smartphones [42], smartwatches [60], fitness trackers [35]. The placement of the sensor on the human body is important for accurately detecting the human's activity, as body parts move differently depending on the activity. For example, movements while sitting cannot be captured if the sensor is placed in the human's pockets [49].

Location information is usually obtained using a GPS sensor, which is interesting for moving humans, as their means of transportation can be detected using the human's speed [74]. Additionally, the geographical context helps infer the activity in which the human is engaged [46]. For example, 30% of traffic in urban areas are due to drivers searching for a parking spot. A system using GPS sensors can detect when a spot has vacated and alert a nearby driver [52].

Finally, physiological signals, e.g., heart rate, respiration rate, and skin temperature, can be used alongside acceleration data to more accurately predict human activity [44]. Activities may have different effects on a human's physiological metrics [43]. For example, the more demanding the activity, the higher the heart-rate and the lower the respiration rate [43].

Recognizing human activities from wearable sensors requires data acquisition. Data is acquired in multiple stages [43]. First, wearable sensors are selected for their suitability to detect a certain actions or activities representative of a task. Second, the wearable sensors are integrated with devices that capture the data. Finally, the data is stored either locally on the integration device or remotely on a server. During the data acquisition process subjects perform a predefined set of activities that the recognition system is later able to detect. After the data is collected, activity recognition consists of two stages, training and testing the activity recognition system, which is described in Chapter 2.3.

2.2.3. Differences

External and wearable sensors differ in regards to privacy, pervasiveness, complexity, mobility, and accuracy. These factors are important for developing a system to detect the medical procedures EMS personnel apply to a patient. Privacy is extremely important in a healthcare environment, which is why the United States has HIPAA [19] and Germany has "Die ärztliche Schweigepflicht" [65]. Pervasiveness is defined as the sensor's ability to be connected or attached to any device and any location [43]. Proper functioning of the automatic detection system requires the system must run in real-time. EMS personnel are usually mobile when performing their duties from initiating patient care to transporting and hand-off at the hospital. Finally, sensor accuracy is critical, as a falsely recognized EMS procedure may have fatal results [51].

Privacy has become a growing societal concern [67]. Patients and EMS personnel may object to constant monitoring using cameras [4]. Over 40% of police leadership think that body-worn cameras are used to "fish" for evidence against their officers [61]. The same problem may occur when EMS personnel are equipped or surrounded by cameras, as the video may be used as evidence of wrong-doing. Wearable sensors may reduce this perception of privacy intrusion, as the wearable sensor is a passive observer without the camera.

Pervasiveness for external sensors is low, because cameras can not be easily attached to humans. The cameras have to be mounted externally and pointed at the human. The monitored human has to stay within a perimeter defined by the position and the field of view of the camera. Inside an ambulance multiple cameras have to be deployed to mitigate the obscureness effect of body parts covering a region of interest [33]. Wearable sensors can capture data the entire time the sensor is worn, while cameras collect more informative data concerning the overall environment and activities that wearable sensors may be unable to detect.

Video processing is extremely computational expensive; therefore, external sensors have high complexity. A Full HD camera with 30 frames per second using the H.264 codec has a data rate of about 8.2 Mbps. The video must be processed to identify the human skeleton using software, such as OpenPose [28]. Real-time video processing requires a

2. Literature Review

high-end graphics card [47]. Wearable sensors capture a different type of data at a different resolution; thus, the wearable sensors have lower complexity than external sensors.

HAR cameras are typically stationary and positioned a priori in order to cover a region of interest [56]. Therefore, the mobility of a video monitoring system is low. A camera's mobility is negligible in the context of detecting procedures in an ambulance, as the environment does not change. Wearable sensors commonly use technology, e.g., Bluetooth, WiFi, to communicate with a processing computer [43]. The mobility of the wearable sensors allows the wearer to maintain his or her range of motion. A downside of wearable sensors' mobility is battery-life [43]. Depending on the device, the battery capacity may be limited and not last through its designed time. Wearable sensors are essential for detecting procedures performed outside of the ambulance. Wearable sensors can connect to a phone on the EMS personnel and collect data anywhere [43].

The accuracy of sensors is dependent on the sensors' hardware and processing. First, the sensor's hardware has to collect the data accurately. Several factors of cameras determine the data's accuracy, such as resolution [22], camera sensor size [8], low-light capabilities [45], etc. Wearable sensor accuracy depends on the sensors' uncertainty of measurement and sampling rate at which data is obtained. Machine Learning systems can use data to train a model to recognize human activities. Recently, visual-based activity recognition accurately detected up to 70.4% [31] of human activities from the human motion database [41]. Every day wearable sensors, such as smartphones can detect jogging, laying, sitting, standing, and walking with a 99.01% accuracy [69]. Wannenborg and Malekian's [69] results are not comparable to Herath, Harandi, and Porikli's [31] result as the datasets were different, but Wannenborg and Malekian showed how far existing Machine Learning algorithms have come in recent years.

Visual-based activity recognition can vary greatly in accuracy, as many external factors, such as lighting can affect the quality of video data [45]. Wearable sensors and external sensors complement each other well [53]. While visual data can capture multiple humans simultaneously, a wearable sensor is limited to a single individual and requires multiple sensors to capture each person. Wearable sensors are highly sensitive to the body part on which they are placed, as accelerometer and gyroscope data will only capture the movement of the monitored limb.

Wearable sensors are an effective tool for recognizing human activity with a low intrusion of privacy [43], low computational expensiveness [43], and their pervasiveness [43].

2.3. Machine Learning within Human Activity Recognition

Machine learning algorithms are trained on data collected from wearable and external sensors to recognize human activity. The body part movements are divided into two categories for the purpose of detecting procedures performed by EMS personnel inside an ambulance: coarse-grained and fine-grained movements. Coarse-grained movements are the broadest way to describe an activity, such as cutting an apple [27]. Fine-grained movements are the anatomic movements involved to perform an activity, such as picking up apple, placing apple, picking up knife, slicing knife through the apple, and returning

knife [27]. The approaches of detecting each movement type are analyzed by examining how the features of the dataset were extracted and what learning methods were used to generate a HAR model. Activity recognition accuracies are compared to determine the effectiveness of the machine learning algorithm. The different machine learning algorithms, their number of features, number of activities detected, the kind of sensors used, and the algorithm's accuracy are listed in Table 2.2.

Table 2.2.: Summary of the Reviewed Machine Learning Algorithms

Algorithm	Paper	Features	Activities	Sensors used	Accuracy
Coarse-grained movements					
k -NN ($k = 1$) k -Star	[69]	29	5	accelerometer	99.01%
sparse representation	[73]	60	9	accelerometer gyroscope magnetometer	96.1%
Fine-grained movements					
random forest	[48]	80	17	accelerometer gyroscope magnetometer barometer GPS microphone	90%
conditional random fields	[54]	24	6	accelerometer gyroscope magnetometer	95.74%
k -NN ($k = 5$)	[7]	8	5	accelerometer gyroscope magnetometer EMG	86%
k -NN ($k = 3$)	[66]	3	17	accelerometer gyroscope EMG	89.2%

2.3.1. Coarse-grained movements

A study by Wannenborg and Malekian (2016) detected everyday physical activities using smartphone accelerometer data by applying a k -nearest neighbor (k -NN) and k -Star machine learning algorithm [69]. Five different activities were recognized: standing, sitting, laying down, walking, and jogging. A three-axis accelerometer sensor on a smartphone placed in ten participant's pants pockets was used to collect the data. Windowing with a

size of 1s and 50% overlap was applied, after normalizing the data. Forty-six features were extracted. The features included the minimum, maximum, mean, and median of every axis, as well as the signal magnitude area (SMA). The 29 highest contributing features were selected to train ten different classifiers. k -NN ($n = 1$) and k -Star achieved the highest classification accuracy, with 99.01%. Wannenborg and Malekian only detected activities related to daily life. The algorithm's limited number of recognized activities is not usable for automatically detecting procedures administered by EMS personnel. The algorithm's high accuracy signifies a good feature extraction and training process, but the activities are not representative of the coarse-grained movements related to administering EMS procedures.

A three-axis accelerometer, three-axis gyroscope, and three-axis magnetometer were used by Zhang and Sawchuk (2013) to recognize nine common activities [73]. Fourteen participants performed the activities: walk forward, walk left, walk right, go upstairs, go downstairs, jump up, run, stand, and sit. The sensors were placed on the participant's hip, and 110 features were extracted, such as mean, median, variance, SMA, etc. The features were selected using sequential forward selection for four classifiers: k -nearest neighbor, naive Bayesian classifier, support vector machine, and sparse representation. The sparse representation classifier achieved the highest accuracy (96.1%) when using 60 features.

The algorithms of Zhang and Sawchuk [73], and Wannenborg and Malekian [69] were able to accurately detect common daily life human activities.. The activities detected in Zhang and Sawchuk's work were broader than those detected by Wannenborg and Malekian. The features extracted were similar, such as using min, max, SMA, etc. Therefore, using accelerometer, gyroscope, and magnetometer to detect common human activities in daily life is highly accurate. The same process of processing data of coarse-grained movement can be applied for recognizing procedures administered by EMS personnel.

2.3.2. Fine-grained movements

A machine learning algorithm developed by Maier and Dorfmeister (2014) detected 17 unique fine-grained activities and transportation phases related to subway travel [48]. The 17 fine-grained movements are: walking in the subway station, walking upstairs/downstairs, using an escalator (up and down without walking, up and down while walking), using an elevator (up and down), waiting, waiting while the subway arrives, entering the subway train, standing in the subway while parking/accelerating/driving/decelerating, and exiting the subway train. The sensors used were accelerometer, gyroscope, magnetometer, barometer, GPS, and microphone. A window of 2 seconds with 50% overlap was applied to the sensor data in order to achieve the highest classifier accuracy. The transitions between activities were ignored. The Fast-Fourier transformation was applied in order to the sensor data to compute frequency-based features, while time-based features, i.e., the maximum and the mean, were computed to generate a total of 632 features. A correlation-based feature subset selection was used to filter the 632 features down to 80 features. The random forest classifier achieved a 90% accuracy with the algorithm's parameters set to their default values. This study shows that fine-grained activities can be accurately detected using the sensors on a smartphone. Microphone data may not be included in a healthcare environment due to privacy concerns.

A wrist worn nine-axis inertial measurement unit (IMU) was used to detect smoking gestures [54]. The IMU device consisted of a three-axis accelerometer, three-axis gyroscope, and three-axis magnetometer. Participants labeled smoking, eating sessions, and "other" using a mobile app. Fine-grained gestures, such as smoking puffs, food bites, and "other" were added a posteriori. Data from 15 participants included 28 hours of 17 smoking sessions, and 10 eating sessions, as well as 369 smoking puffs and 252 food bites. Data labeled "other" was not used in classification. A conditional random field classifier achieved 95.74% accuracy in detecting smoking puffs and food bites using the data from a ten second window. The system differentiated very similar gestures; however, only two activities were considered. Many different gestures occur in the context of an EMS personnel performing procedures inside of an ambulance.

A Myo armband was used to detect hand gestures [7], which included: fist, open hand, wave hand in, wave hand out, pinch fingers, and no gesture. Electromyography (EMG) data was captured at 200 Hz and pre-processed by taking the absolute value of all of the EMG channels followed by a Butterworth filter to reduce noise and smooth each channel. A 2-second window with an overlap of 50% was applied to the EMG data, which generates 400 samples. The k -nearest neighbor rule and the dynamic time warping algorithm was used to recognize the hand gestures and achieved an accuracy of 86%. Myo's proprietary hand gesture recognition only achieves an accuracy of 83% [7]. Processing the data prior to algorithmic inclusion may be useful for detecting fine-grained movements by EMS personnel when performing procedures on patients.

Using data from the Myo armband, Totty and Wade (2017) trained a k -NN machine learning algorithm to detect upper-extremity activities [66]. Gestures were categorized and split into tasks with an approach used by the Functional Arm Activity Behavioral Observation System [68]. Ten participants performed 17 upper-extremity tasks: arm swaying during walking, assisted movement, touching face, scratching leg, waving, covering yawn, holding object, adjusting arm position, reaching, grabbing, wiping a table, moving an object, transferring an object from hand-to-hand, pushing up from a seated position, wiping a table hurriedly, waving excitedly, and scrubbing. The accelerometer and gyroscope data were smoothed using a 4th order Butterworth band-pass filter, and the EMG data was high-pass filtered. The features included the mean and the SMA of the acceleration and gyroscope data, and the root mean square (RMS) of the EMG data. Data from the magnetometer was not used on the algorithm, due to the sensor's susceptibility to environmental noise [2]. The k -NN classifier achieved an accuracy of 89.2%.

Compared to the first Myo study, Totty and Wade detected activities, such as holding an object, reaching, and grabbing may be useful in the context of medical procedure detection. In the medical context an EMS personnel frequently reaches and grabs tools inside an ambulance. The feature extraction and pre-processing methods can be used as a basis for data collected in a study.

2.3.3. Intention Recognition

A human's motion can be characterized using the sequence of movements [27]. For example, EMS personnel placing an oral airway have to place a thumb on the bottom teeth

2. Literature Review

and index finger on the patient's upper teeth, then move the fingers outward, insert the airway into the patient's mouth, and finally rotate the airway 180 degrees.

The human's sequence of actions can be used to predict the next intended action [59]. Recognizing the human's intention based on the motion trajectories is proposed by Huang, Jiang, Chui, and Jiang [71]. A stacked Hidden Markov Model was trained to recognize the primitive and subtask level during virtual laparoscopic cholecystectomy surgery. The four subtasks were: ablation of the connective tissue and dissection of the cystic duct, checking the clearance between the cystic duct and the liver, deployment of three clips on the cystic duct, and division of the cystic duct. The motion primitive layer considers the motion of both hands individually. Twelve participants performed the virtual surgery ten times. The processing window was 0.5 seconds with 80% overlap. The recognition rate was 71% for the subtask level and 95% for the primitive level. A recognition rate as low as 71% is impractical when automatically detecting procedures performed by EMS personnel. The intention recognition system only differentiated between four subtasks, while EMS perform many different subtasks in an ambulance.

A Hybrid Dynamic Bayesian Network was used to recognize the intended coarse-grained movement [26]. The probability density over all classes was represented using a continuous density function. The recognition system was tested using seven kitchen activities captured on video: set the table, prepare cereal, prepare pudding, eat with a spoon, eat with a fork, clear the table, and wipe the table. The average recognition rate was 74.4% for the test set. An intention recognition system can send the hospital information regarding the procedure that may be performed next on the patient, while the treatment is still in progress. Communicating time-critical information about the current treatment allows the emergency department to prepare accordingly, before patient arrival.

2.3.4. Discussion

Distinguishing between coarse-grained and fine-grained movements is important in the context of detecting procedures administered by EMS personnel on a patient inside of an ambulance. Many procedures include similar fine-grained movements, which can lead to misclassification. Therefore, procedure recognition must account for both types of movement during classification.

Most algorithms followed the same approach for feature extraction and processing data. This approach of taking a window with 50% overlap, reducing noise with a 4th order Butterworth band-pass filter, and calculating mean, median, variance, SMA, etc. can be applied to data for automatically recognizing procedures administered by EMS personnel. Data from EMS personnel administering procedures needs to be pre-processed to reduce noise and calculate more meaningful metrics. The window size applied to the data depends on the length of a given activity, while existing research shows a 50% overlap as the most accurate [69].

An IMU is good at detecting fine-grained movements [54]. The IMU's accelerometer, gyroscope, and magnetometer have successfully detected coarse-grained movements [73]. The Myo, which incorporates acceleration, gyroscope and magnetometer, is useful for detecting muscle activation on a human's arm. The Myo has been proven to be accurate in detecting fine-grained human activities [7]. A procedure administered by EMS personnel

consists of many fine-grained movements. Through detecting the fine-grained movements using the Myo, the procedures can be predicted. The existing literature uses similar approaches to feature extraction and data processing, which can be applied in the context of automatically detecting EMS procedures.

2.4. Summary

External and wearable sensors were examined and compared for their applicability in the medical field. Combining an external sensor with wearable sensors may achieve the highest accuracy for detecting human activities. Human activities consist of coarse-grained and fine-grained movements. Several machine learning algorithms that use wearable sensor data can accurately detect human activities. Inferring coarse-grained movements from fine-grained movements may be useful in the context of detecting procedures administered by EMS personnel inside an ambulance.

3. Methodology

The approach to developing an automatic system capable of detecting procedures administered by EMS personnel consists of breaking the procedures into anatomical movements, developing an algorithm, and collecting data to train the algorithm through a user study. This thesis focuses on automatically detecting five EMS procedures: placing a intravenous tourniquet, wrapping a wound, applying a bag-valve-mask, placing an oral airway, and CPR (Figure 3.1). The five EMS procedures were chosen for their reproducibility on a demo mannequin and their assumed recognition difficulty. CPR is assumed to be easily recognizable, due to the repetitive motion during compressions in the accelerometer data. Bag-valve-mask application is assumed to be easily recognizable, due to the repetitive motion during squeezing the bag in the EMG data. Placing a tourniquet is assumed to be harder to recognize, due to missing repetitive motion. Wrapping a wound is assumed to be harder to recognize, due to missing repetitive motion. Placing an oral airway is assumed to be the hardest to recognize, due to missing repetitive motion and a short duration.

3.1. Hierarchical Task Analysis

Medical procedures include repetitive and unique movements. Distinctive patterns in the data from repetitive and unique movements help machine-learning algorithms achieve higher performance. Therefore, the EMS procedures are broken into their anatomical movements using *Hierarchical Task Analysis* in order to identify distinctive patterns in the EMS procedures [38]. The Hierarchical Task Analysis divides tasks (procedures) into sub-tasks, followed by sub-sub-tasks, and finally anatomical movements. The resulting anatomical movements are analyzed to include their sensability using five commercially available sensors: Apple Watch, Myo, Empatic E4, Garmin Watch Forerunner, and Biopac Bioharness BT. Sensability is the ability of a sensor to recognize a human movement. The

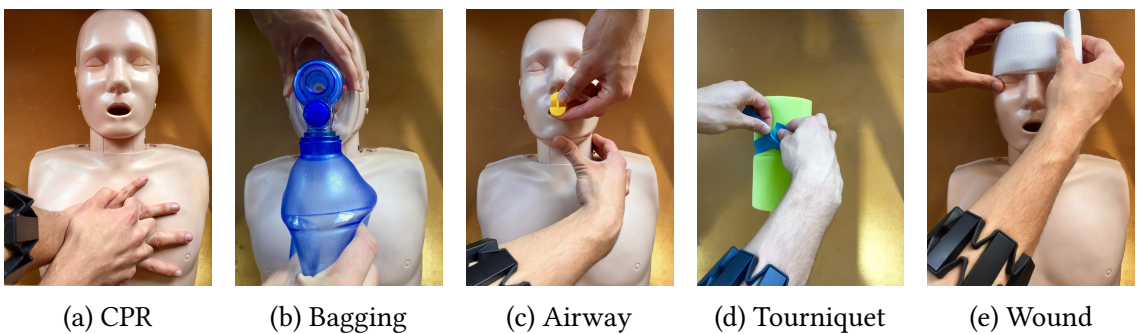


Figure 3.1.: EMS procedures

3. Methodology

sensability is determined by considering the type of sensor data and the sensors' ability to detect anatomical movements, such as recognizing muscle movement through EMG data. The placement of a sensor is crucial in its ability to detect anatomical movements. The EMG data for the hand is captured by placing the sensor on the arm. Table 3.1 displays an overview of the procedures with their respective sensability per sensor. The rows present the procedures with their number of sub-tasks, multi-hand sub-tasks, task movements, and unsensed task movements. Multi-Hand sub-tasks are sub-tasks that require more than one hand to complete.

Task	# Sub-Tasks	# Multi-Hand Sub-Tasks	# Task Movements	# Unsensed Task Movements	% Sensed Apple Watch	% Sensed MYO	% Sensed Empatic E4	% Sensed Garmin Forerunner	% Sensed Bioharness BT
CPR	5	4	36	7	39%	61%	39%	39%	19%
Bagging	5	2	27	1	48%	96%	48%	48%	0%
Oral Airway	4	1	16	0	50%	100%	50%	50%	0%
Place a Tourniquet	2	2	7	0	71%	100%	71%	71%	0%
Wrapping a wound	2	3	6	0	83%	100%	83%	83%	0%

Table 3.1.: Hierarchical Task Analysis: Overview

CPR is a procedure that is performed on patients with cardiac arrest to preserve brain functionality. The Hierarchical Task Analysis of CPR (Table A.1) resulted in four sub-tasks, with two ways to perform the giving breaths sub-task. The first sub-task is to lift the patient's chin, then check for breathing. If the patient is not breathing, there are two ways to give breaths: mouth-to-mouth (Sub-Task 1.3A) and using a bag-valve-mask (Sub-Task 1.3B). The study uses the bag-valve-mask to ventilate the patient, as the mask is commonly used by EMS personnel. After giving two breaths, 30 chest compressions are performed. The breaths and compressions are repeated until the patient has stabilized. CPR contains 27 anatomical task movements when a bag-valve-mask is used to ventilate the patient, of which five were determined not to be sensible using the commercial sensors. The Myo is capable of detecting 22 anatomical tasks, 14 more than the other commercial sensors. Compared to the other devices, the Myo is the only device that includes an EMG sensor, which makes it better at detecting anatomical tasks.

Bag-Valve-Mask ventilation is a procedure used to artificially breath air into a patient's lungs. A bag full of air is attached to a mask, which allows for airflow to the patients' mouth and nose when the bag is squeezed. Hierarchical Task Analysis of Bag-valve-mask ventilation (Table A.2) resulted in four sub-tasks, with two ways to place an airway. The first sub-task for EMS personnel is to raise the gurney level for easier access, then the patient's chin is lifted. If the patient is unresponsive an oral airway is placed, otherwise a nasal airway is placed. This thesis uses oral airways, as the demo mannequin does not

feature a nasal canal. However, the algorithm can be extended to detect the use of a nasal airway. Finally, the patient is ventilated using the bag-valve-mask by squeezing the bag, pushing air into the patients' lungs. A total of 26 anatomical task movements were found, of which one was determined to not be sensable using the commercial sensors. The Myo is capable of detecting 25 anatomical tasks, eight more than the other commercial sensors.

Placing an intravenous tourniquet is a procedure to highlight veins for better needle placement by constricting blood flow. Hierarchical Task Analysis of placing an intravenous tourniquet (Table A.4) resulted in two different sub-tasks. At first an EMS personnel has to grab a tourniquet. Then, the tourniquet is applied by tying it around the arm. A total of seven anatomical task movements were found, of which all were determined to be sensable using the Myo, two more than the other commercial sensors.

Wrapping a wound is a procedure to stop bleeding of an open wound. Hierarchical Task Analysis of wrapping a wound (Table A.5) resulted in two sub-tasks. At first an EMS personnel has to grab the pressure dressing. Then, the pressure dressing is placed on the wound and wrapped around it. A total of five anatomical task movements were found, of which all were determined to be sensable using the Myo, one more than the other commercial sensors.

The Myo was chosen as the wireless sensor for the study due to its capability to sense the majority of the anatomical movements. Two Myo devices expands the coverage for data collection to both arms, which is useful in detecting multi-hand tasks.

Task recognition results in higher accuracy when each procedure has unique movements, as there are significant changes in patterns [37]. The five procedures include two unique sub-tasks: compression for CPR, and ventilating the patient for bag-valve-mask ventilation. There are several overlapping sub-tasks:

- **squeezing a bag** for CPR, and bag-valve-mask ventilation;
- **lifting a patient's chin** for bag-valve-mask ventilation, and placing an oral airway;
- **moving the valve mask into position** for CPR, and bag-valve-mask ventilation;
- **grabbing the valve mask** for CPR, and bag-valve-mask ventilation;
raising the patient for bag-valve-mask ventilation, and placing an oral airway;
- **placing an oral airway (oropharyngeal)** for bag-valve-mask ventilation, and placing an oral airway;

Overlapping sub-tasks have to be treated with caution as they solely cannot directly identify a procedure. The unique sub-tasks may be clear indicators that the procedure associated with that sub-task is being performed, while overlapping sub-tasks are not clear indicators. Therefore, when a unique sub-task is detected it is safe to reliably infer the associated procedure, while an overlapping sub-task requires further sub-tasks in the sequence.

3. Methodology

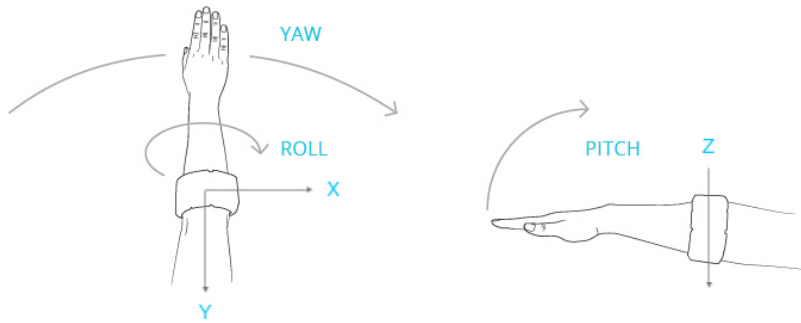


Figure 3.2.: Myo Reference Frame (Source: <http://developerblog.myo.com/gui-without-going-beyond-screen-myotm-armband/>)



Figure 3.3.: Myo Gestures (Source: <https://dribbble.com/shots/1937560-Gesture-Icons>)

3.2. Algorithm

The algorithm to recognize procedures performed by EMS personnel inside an ambulance relies on acceleration, gyroscope, and EMG data. Human activity recognition algorithms have been proven to accurately detect activities when using acceleration, gyroscope, and EMG data [66, 7].

3.2.1. Data Acquisition

Acceleration, gyroscope, and EMG data are acquired through the Myo armband. The Myo armband is created by Thalmic Labs, Inc. and includes an EMG sensor, triaxial accelerometer, a triaxial gyroscope, and triaxial magnetometer. The data from the magnetometer is not used in the algorithm, due to its susceptibility to environmental noise [2]. Acceleration and gyroscope data is available at 50Hz, while EMG data is available at 200Hz. The EMG data has eight channels with 8bits of resolution for each channel. The accelerometer data consists of x , y , and z values, and the gyroscope data has *roll*, *pitch*, and *yaw* (Figure 3.2). The Myo's z axis is perpendicular to the floor, while the x and y axis are in the plane relative to the floor. The Myo's *pitch* axis is rotating the arm up and down, the *yaw* axis is rotating the arm side to side, and the *roll* axis is rotating the arm along itself. Finally, the Myo has an output for proprietary hand gesture recognition, which is used as a feature for the algorithm (Figure 3.3): pinch, fist, open, wave in, and wave out.

3.2.2. Data Processing

The data from the acceleration, gyroscope, and EMG sensors needs to be processed in order to reduce noise and motion artifacts. Accelerometer and gyroscope data is smoothed using

a 4th order Butterworth band-pass filter with cut-off frequencies at 0.2Hz and 15Hz [39]. The EMG data is high-pass filtered at 20Hz to reduce motion artifacts, as recommended in related works [21].

3.2.3. Feature Extraction

Human activity recognition systems take features extracted from processed data as input. The features are calculated through the use of a sliding window. Due to the time it takes to perform different anatomical movements, the window size will have a length of 2s [48]. The window will have a 50% overlap, which has been proven sufficient in related work [69]. Table 3.2 displays all calculated features: Mean, standard deviation, and signal magnitude area for the IMU; Mean, signal magnitude area, root mean squared, and power spectral density for EMG. *Mean acceleration*, given in Equation 3.1, is calculated by excluding the

	Domain	Features
IMU	Time	Mean
		Standard deviation
		Signal Magnitude Area
EMG	Time	Mean
		Signal Magnitude Area
		Root Mean Squared
	Frequency	Power Spectral Density

Table 3.2.: Features for the Machine Learning algorithm

highest and lowest 10% of the data, taking the sum of each of the three accelerometer axes and dividing by the number of values [66]. Excluding the outliers removes any spikes that may occur due to collisions. The mean acceleration is calculated as \overline{acc}^{axis} , where *axis* represents all three axes *x*, *y*, *z* and *N* is the number of acceleration values. The values for acc_i^{axis} include the data for an entire procedure, excluding the highest and lowest 10%.

$$\overline{acc}^{axis} = \frac{1}{N} \sum_{i=1}^N acc_i^{axis} \quad (3.1)$$

The mean acceleration feature was chosen to represent the quantity of motion [3]. *Acceleration Standard deviation*, given in Equation 3.2, is a measure describing the variance in a set of axis values. The calculated value is represented as $acc_σ^{axis}$, where *axis* represents all three axes *x*, *y*, *z* and *N* is the number of acceleration values.

$$acc_σ^{axis} = \sqrt{\frac{\sum_{i=1}^N (acc_i^{axis} - \overline{acc}^{axis})^2}{N - 1}} \quad (3.2)$$

Acceleration signal magnitude area acc_sma, given in Equation 3.3, is computed by dividing the numerically-integrated area under the curve by the duration of the signal [66]. The value of the axes are acc_x , acc_y , acc_z respectively, and *T* is the time duration of the signal.

$$acc_sma = \frac{1}{T} \int_0^T (|acc_x| + |acc_y| + |acc_z|) dt \quad (3.3)$$

3. Methodology

The signal magnitude area of the acceleration feature was chosen, because it represents the gross motion of movements and the energy expenditure [34]. *Mean angular rate of change*, given in Equation 3.4, is calculated by taking the sum of each of the three gyroscope axes *yaw, pitch, roll* and dividing by the number of values N [66].

$$\overline{gyro}^{axis} = \frac{1}{N} \sum_{i=1}^N gyro_i^{axis} \quad (3.4)$$

The mean rate of change feature was chosen, because it represents the quantity of rotation. *Rate of change standard deviation*, given in Equation 3.5, is a measure describing the variance in a set of axis values. The calculated value is represented as $gyro_{\sigma}^{axis}$, where *axis* represents all three axes *yaw, pitch, roll* and N is the number of acceleration values.

$$gyro_{\sigma}^{axis} = \sqrt{\frac{\sum_{i=1}^N (gyro_i^{axis} - \overline{gyro}^{axis})^2}{N - 1}} \quad (3.5)$$

Angular rate of change signal magnitude area, given in Equation 3.6, is calculated by dividing the numerically-integrated area under the curve by the duration of the signal [66]. The value of the axes are $gyro_{yaw}$, $gyro_{pitch}$, $gyro_{roll}$ respectively, and T is the time duration of the signal.

$$gyro_{sma} = \frac{1}{T} \int_0^T (|gyro_{yaw}| + |gyro_{pitch}| + |gyro_{roll}|) dt \quad (3.6)$$

The angular rate of change signal magnitude area feature was chosen, because it represents the gross rotation of movements.

Mean muscle activation $\overline{emg}^{channel}$, given in Equation 3.4, is calculated by taking the sum of each of the eight EMG channels and dividing by the number of values N .

$$\overline{emg}^{channel} = \frac{1}{N} \sum_{i=1}^N emg_i^{channel} \quad (3.7)$$

The mean muscle activation feature was chosen, because it represents the quantity of muscle movement. *Muscle activation signal magnitude area*, given in Equation 3.8, is calculated by dividing the numerically-integrated area under the curve by the duration of the EMG signal. The EMG channels are represented as $e1, \dots, e8$ and T is the time duration of the signal.

$$emg_{sma} = \frac{1}{T} \int_0^T (|e1| + |e2| + |e3| + |e4| + |e5| + |e6| + |e7| + |e8|) dt \quad (3.8)$$

Muscle activation root mean squared is calculated for each of the eight EMG channels and then averaged. Equation 3.9 calculates the root mean squared for every channel $i = 1, \dots, 8$, where N represents the number of values. Equation 3.10 calculates the final averaged root mean squared value of all channels.

$$emg_{channel_i_{rms}} = \sqrt{\frac{1}{N} (emg_{channel_i_1^2} + \dots + emg_{channel_i_N^2})} \quad (3.9)$$

$$root_mean_squared = \frac{1}{8} \sum_{i=1}^N emg_channel_i_{rms} \quad (3.10)$$

Root mean squared is proven to be the gold standard for EMG-force analysis [36]. The root mean squared value represents physiological activity during contraction of the muscle [66]. *EMG Fast Fourier transformation* is applied to each EMG channel to transform the signal from the time domain into the frequency domain. Power Spectral Density represents the distribution of signal strength, which is taken from the frequency domain. The frequency spectrum can be used to detect muscle fatigue, force production and muscle fiber signal conduction velocity [29].

3.2.4. Machine Learning

The machine learning algorithm approach trains a separate Hidden Markov Model (HMM) for every EMS procedure. HMMs in human activity recognition are based on modeling human activity as first-order Markov chains. A Markov chain represents a discrete time stochastic process covering a finite number of states, where the current state depends on the previous state [14]. Every coarse-grained movement is represented by a state for EMS procedures, while one HMM model corresponds to the procedure. The Figure 3.4 shows how each procedures is divided into its coarse-grained movement as state for the HMM. An observation sequence is tested by putting the data into each model and calculating the likelihood of the observation. The model with the highest likelihood is the class for the observation. A HMM λ is represented as $\lambda = (A; B; \pi)$, where A is the transition matrix, B is the observation matrix, and π is the initial probability array. S , given in Equation 3.11, is the state alphabet set, in this case hidden. V , given in Equation 3.12, is the observation alphabet set, such as the data we collect from the sensors [16].

$$S = (s_1, s_2, \dots, s_N) \quad (3.11)$$

$$V = (v_1, v_2, \dots, v_M) \quad (3.12)$$

Q , given in Equation 3.13, is the fixed state sequence. O , given in Equation 3.14, is the corresponding observation.

$$Q = q_1, q_2, \dots, q_T \quad (3.13)$$

$$O = o_1, o_2, \dots, o_T \quad (3.14)$$

A , given in Equation 3.15, is the transition matrix containing the probability of state j following state i .

$$A = \{a_{ij} = P[q_t = s_j | q_{t-1} = s_i]\}, 1 \leq i, j \leq M, \sum_{j=1}^N a_{ij} = 1 \quad (3.15)$$

B , given in Equation 3.16, is the observation matrix containing the probability of observation k being produced from the state j .

$$B = \{b_{jk} = P[o_t = v_k | q_t = s_j]\}, \sum_{k=1}^M b_{jk} = 1 \quad (3.16)$$

3. Methodology

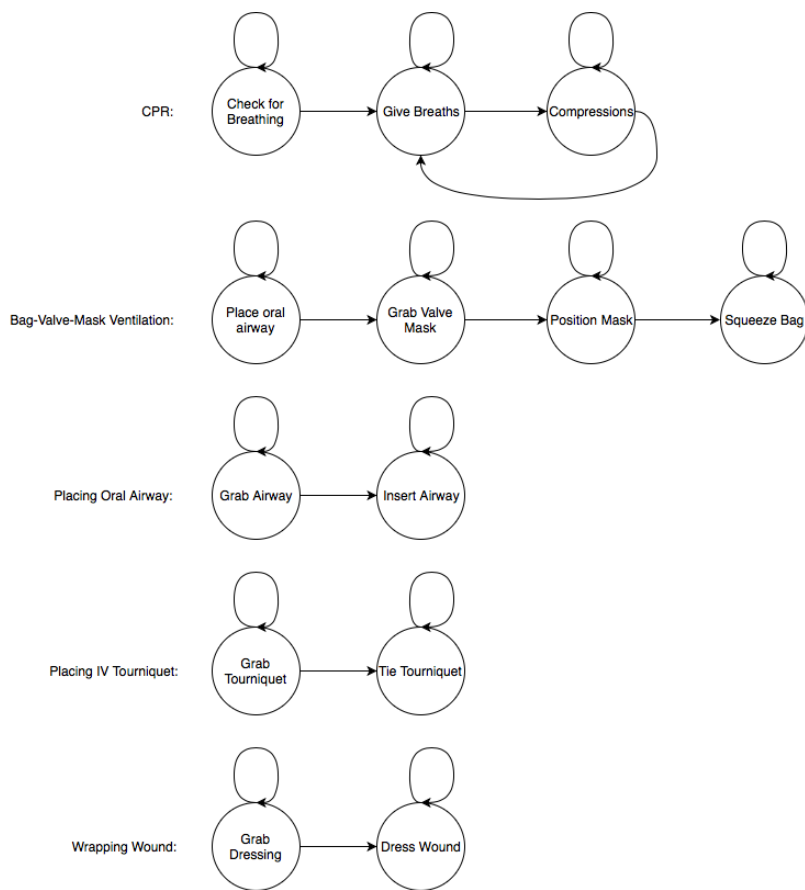


Figure 3.4.: HMM state diagram for EMS procedures

π , given in Equation 3.17, is the initial probability array.

$$\pi = [\pi_i], \pi = P(q_1 = s_i) \quad (3.17)$$

HMMs can be trained in two different ways: unsupervised and supervised. Supervised training is done, when a dataset is given with labels corresponding to every state of a HMM. The training data is labeled according to the EMS procedures to differentiate between the different HMMs. The HMMs are trained unsupervised with a predetermined number of states determined by from the Hierarchical Task Analysis using the Baum-Welch algorithm. The Baum-Welch algorithm is a strict version of the Expectation-Maximization algorithm, meaning the Baum-Welch algorithm is guaranteed to converge to at least a local maximum [6]. The output of the Baum-Welch algorithm is the most likely hidden transition probabilities A and the most likely set of emission probabilities B . The modeled HMMs λ_j for the EMS procedures $j = 1, \dots, 5$. Given a test sequence, Y , the probability for every HMM is calculated as follows:

$$P_j = \log(P(Y|\lambda_j)), j = 1, \dots, 5.$$

The result of the classification is taking the highest probability of all HMMs:

$$\lambda^* = \max_j \{P(Y|\lambda_j)\}.$$

3.3. Experimental Design

A machine learning algorithm needs data from different people performing all five procedures a number of times in order to be trained. The following chapter describes a study design to collect data from participants for the automatic recognition system.

3.3.1. Data Collection

The study was designed to be within-subjects and consists of two questionnaires, training, and data collection. The first questionnaire asks for the participant's demographics, such as: age, gender, education, handedness, and the amount of exercise per week. The second questionnaire evaluates the participant's state of fatigue, such as: the amount of caffeine intake, hours of sleep the last night, hours of sleep the night before, feeling of fatigue as Likert scale, and feeling of stress as Likert scale. The study is split into three days and structured as follows:

1. **Day 1** (1 hour): First, the participant was asked to sign the consent form. Then, after a brief introduction to the experiment, the participant was fitted with two Myos on each of his or her arms. Next, the participant was asked to complete the demographic questionnaire, and the fatigue questionnaire. The remainder of the time, the participant was trained in the five medical procedures: CPR, wrapping a wound, tying a tourniquet, placing an oral airway, and bag-valve-mask ventilation.

3. Methodology

2. **Day 2** (1 hour): After the participant was fitted with two Myos on each of his or her arms, he or she completed a fatigue questionnaire. For the remainder of the time, the participant was trained in the five medical procedures.
3. **Day 3** (1 hour): After the participant was fitted with two Myos on each of his or her arms, he or she completed the fatigue questionnaire. For the first 15 mins, the participant was reminded of the training in the five medical procedures. After a five minute break the participant was asked to complete all five procedures for a minute each with 5 minute breaks in between each procedure, to reduce the impact of fatigue. Finally the participant was asked to do four rounds of completing all five procedures in a sequence: placing a tourniquet, wrapping a head wound, bag-valve-mask ventilation, placing an oral airway, and performing cpr with a 5 minute break between each round.

3.3.2. Participant Demographics

The participant's mean age was 23.4 (St. Dev. = 4.72), where 60% were female and 40% were male. Most participants (80%) completed some college degree, 10% have a Masters degree, and 10% have a Doctorate degree. The participants were primarily right-handed (90%), with 10% left-handed. The participant's mean amount of exercise was 4.5 per week (St. Dev. = 1.89).

3.3.3. Machine Learning

The machine learning algorithm approach is compared to three different machine learning algorithms: SVM, decision-tree, and k -NN. SVMs work by constructing hyperplanes between classes. SVMs use different kernel functions to define the hyperplane, such as: linear, polynomial, and Gaussian radial basis function. The comparison will use the radial basis function, as the problem is non linear and it is the de facto standard. A decision-tree is a graph in which each node compares data values to a condition, a branch follows the result of the comparison, and each leaf is the class label. Finally, k -NN is an algorithm where the inputs are the k closest neighbors of the data point. The algorithm counts the class label of each label and determines the label of the data point using majority voting.

3.3.4. Research Questions

The evaluation of the automatic recognition system focuses on the accuracy of the machine learning algorithm, in order to evaluate two hypotheses:

- H_1 : Recognition of CPR and Bag-valve-mask ventilation will have the highest accuracy for each machine learning algorithm, due to its unique movements.
- H_2 : The recognition of a procedure through the sequence of fine-grained movements using a Hidden Markov Model will be more accurate than detecting through training coarse-grained movement models.

4. Results

The machine learning algorithm analysis focuses on the algorithm's ability to detect EMS procedures and generalize across populations. First, the raw EMG and IMU data is presented in Section 4.1. The algorithm analysis for CPR, Bag-Valve-Mask Ventilation, placing an oral airway, placing an IV tourniquet, and wrapping a head wound is presented second in Section 4.2, followed by the population generalizability in Section 4.3.

The machine learning algorithms' ability to detect EMS procedures is analyzed using F1 score, precision, and recall values. Precision is a metric that determines how accurate a model is by taking the fraction of the true positives and dividing it by the predicted positives, given in Equation 4.1. True positives are the number of items correctly labeled as belonging to the positive class and false positives are items incorrectly labeled as belonging to the positive class.

$$Precision = \frac{TruePositives}{TruePositives + FalsePositives} \quad (4.1)$$

Recall is a metric that determines how many of the actual positives the model captures through labeling it as positive, given in Equation 4.2.

$$Recall = \frac{TruePositives}{TruePositives + FalseNegatives} \quad (4.2)$$

F1 score is a metric that combines the precision and recall metric to seek a balance between the two, given in Equation 4.3.

$$F1score = 2 * \frac{Precision * Recall}{Precision + Recall} \quad (4.3)$$

The F1 scores were generated using k-fold cross validation, where k is the number of datasets. Cross-validation varies the training and testing set to produce a more accurate representation of how the algorithm will perform in unseen scenarios. Varying the training and testing set prevents the model from overfitting. Overfitting occurs when the algorithm is unable to perform well in scenarios for which it was not trained on.

The HMM classifier's performance is compared to three different machine learning algorithms: SVM, decision-tree, and k -NN. The algorithms' generalizability is analyzed by leave-one-participant-out cross validation, where the algorithm is trained on 9 participants and tested on the last.

The machine-learning algorithms' hyper-parameters are tuned to improve the accuracy, where the parameters are provided in Appendix A.1

Three window sizes were investigated: 2 seconds, 4 seconds, and 6 seconds, in order to improve recognition for procedures with similar movements. The F1 score improved for all machine learning algorithms by an average of 5% when setting the window size to 6 seconds. The results for a window size of 2 seconds and 4 seconds can be found in Appendix A.2. The following results were calculated using a window size of 6 seconds.

4. Results

4.1. IMU and EMG Patterns

CPR is a procedure that consists of chest compressions and giving breaths in order to resuscitate a patient who is in cardiac arrest. The participants took an average of 56.69 seconds (St. Dev. = 3.76) to complete the CPR procedure. There were seven instances of CPR per participant on Day 3, resulting in a total of 70 instances.

CPR contains several unique movements, which are detected by the IMU and EMG sensors. The first unique movement when performing CPR are the chest-compressions, which are prominent in the IMU sensor data, as seen in Figure 4.1. The acceleration for both hands have sinusoidal peaks with the greatest magnitude on the Myo's X-axis, which is the up-and-down motion from the arms. During the chest compressions, the arm's orientation did not change, nor is there any significant observation in the EMG sensor. The second unique movement occurred when the participant was giving two breaths to the mannequin, as seen in the EMG graph in Figure 4.2. Specifically, the process of giving two breaths presents itself as spikes in the EMG channels: three, four, five, and seven. These spikes can be seen at the beginning and in the middle of the corresponding EMG channel graphs in Figure 4.2. The right hand's orientation also shows two spikes where the two breaths are given.

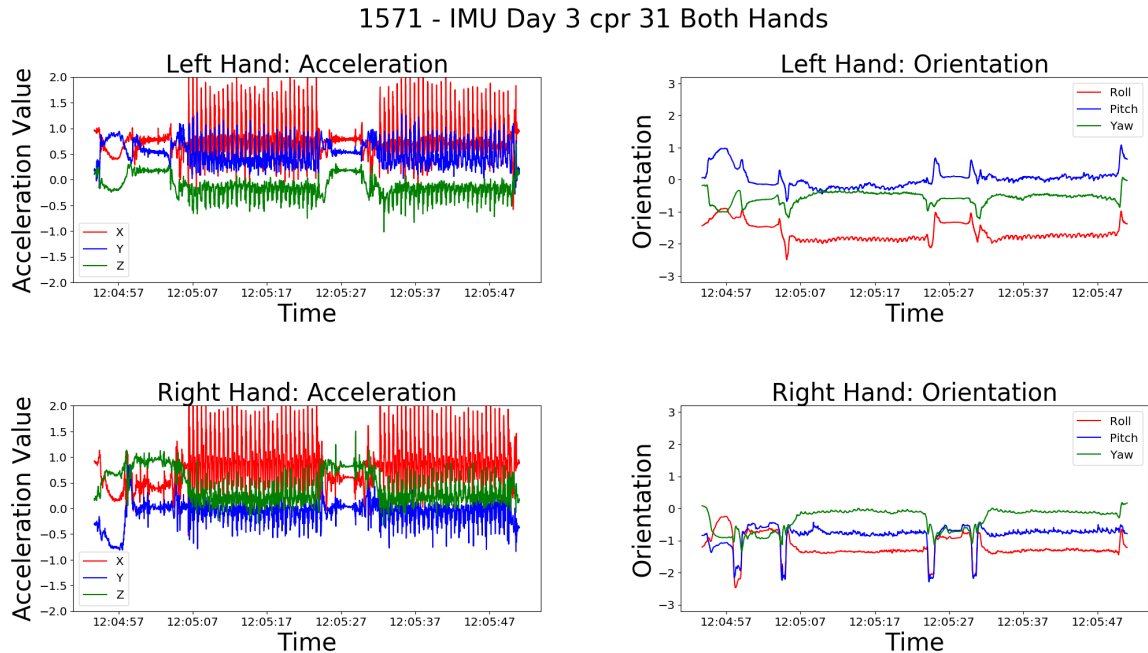


Figure 4.1.: IMU Data Plots for Acceleration and Orientation Data for CPR

Patients without adequate breathing are administered Bag-Valve-Mask ventilation. Completing one round of the Bag-Valve-Mask ventilation procedure took the participants an average of 35.39 seconds (St. Dev. = 5.70). The participants completed two rounds within one minute. The amount of instances for the third day were seven per participant, resulting in a total of 70 datasets.

The bag-valve-mask ventilation datasets consists of the unique squeezing the bag motion in the EMG sensor graph. The periodic motion is visible in all eight EMG channels in

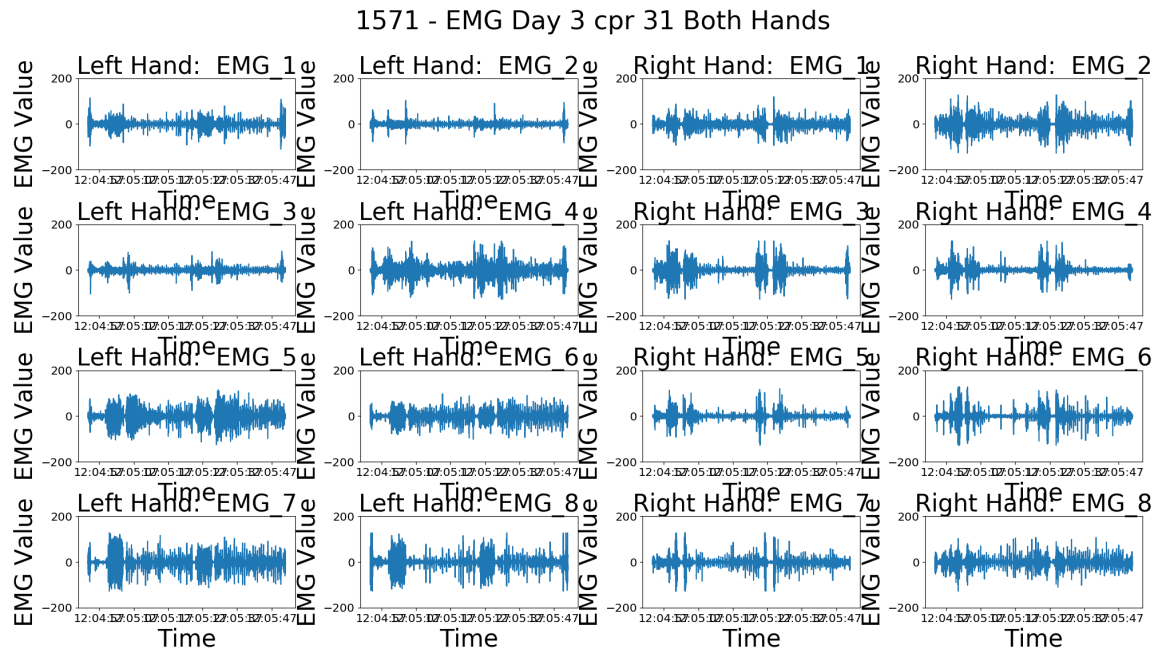


Figure 4.2.: EMG Data Plots for CPR

Figure 4.3. There was no prominent signal in the IMU data, as the right and left hands were stationary during this procedure. Figure 4.4 shows almost flat lines for acceleration and orientation of both hands.

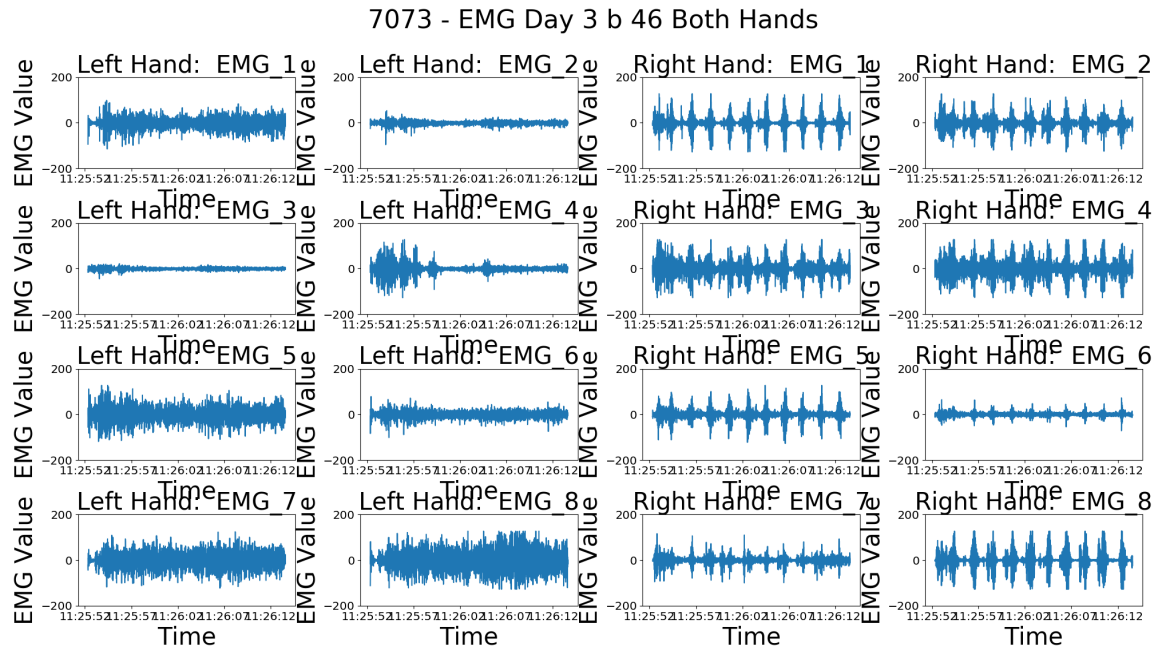


Figure 4.3.: EMG Data Plots for Bag-Valve-Mask ventilation

Placing an oral airway is part of the airway management procedures to prevent and relieve airway obstruction. The participants took an average of 6.51 seconds (St. Dev. =

4. Results

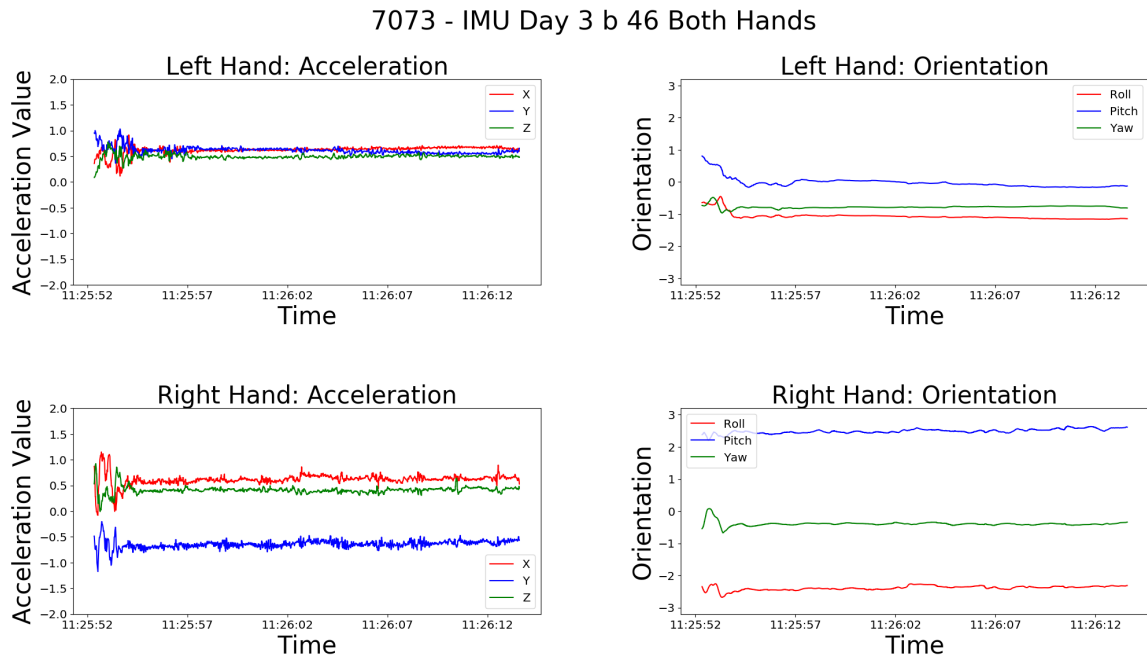


Figure 4.4.: IMU Data Plots for Acceleration and Orientation Data for Bag-Valve-Mask ventilation

2.23) to place an oral airway. The participants were able to complete an average of four rounds within one minute. The amount of instances for the third day were about 9 per participant, resulting in a total of about 90 instances.

Placing an oral airway requires the unique motion of rotating the oral airway 180 degrees after being inserted into the mouth. The rotating motion is visible in the right hand orientation graph starting at 15:14:32 with the bulge of the blue and red line in Figure 4.5. The acceleration data did not show any significant shapes of distribution. The EMG data in Figure 4.6 shows a spike in channels three, four, and five when the oral airway is rotated.

An intravenous tourniquet is used to restrict blood flow on a patient. The participants took an average of 9.38 seconds (St. Dev. = 2.70) to place an intravenous tourniquet. The participants were able to complete an average of three rounds within the one minute data collection of every procedure. The amount of instances for the third day were seven per participant, resulting in a total of 70 datasets.

The placing of an intravenous tourniquet consists of a single wrapping motion around the arm and tying of the ends. The wrapping and tying motion was visible in the IMU's orientation data starting at 9:09:09 with periodic movement and finishing at 09:09:15 with a spike in Figure 4.7. The acceleration and EMG in Figure 4.8 data do not show any significant pattern.

Wrapping a head wound is used to bandage a bleeding on a patient's head. Completely wrapping a head wound took participants an average of 37.26 seconds (St. Dev. = 11.72). The participants were able to complete two rounds within the one minute. The amount of instances for the third day were seven per participant, resulting in a total of 70 instances.

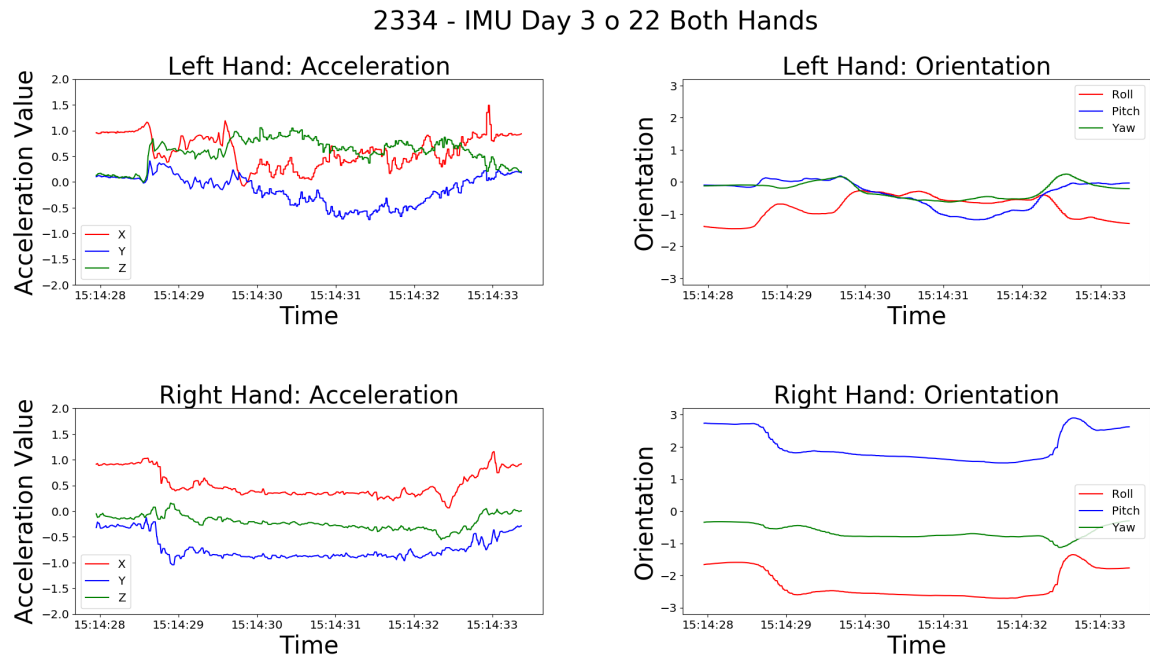


Figure 4.5.: IMU Data Plots for Acceleration and Orientation Data for Placing an Oral Airway

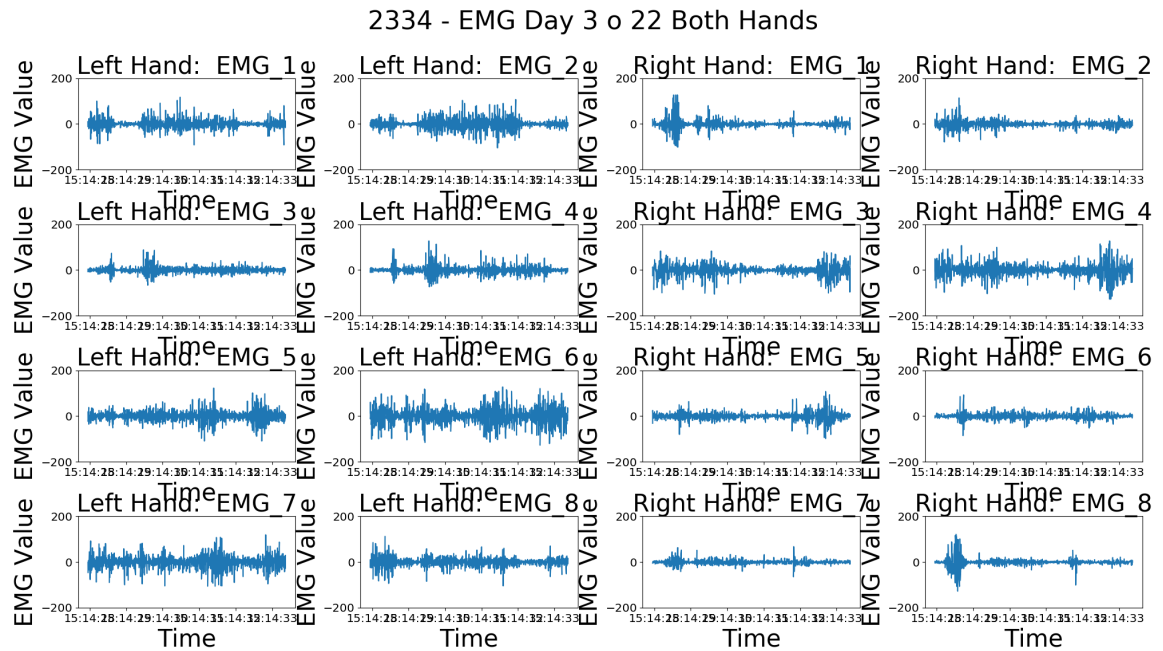


Figure 4.6.: EMG Data Plots for Placing an Oral Airway

The Wrapping of a head wound consists of the unique movement of bandaging around the head of a patient. The wrapping motion is primarily visible in the orientation data of the IMU in Figure 4.9. The spikes in the orientation data at 15:27:18 are sinusoidal and represent the amount of rotations around the head. The EMG data in Figure 4.10 shows a

4. Results

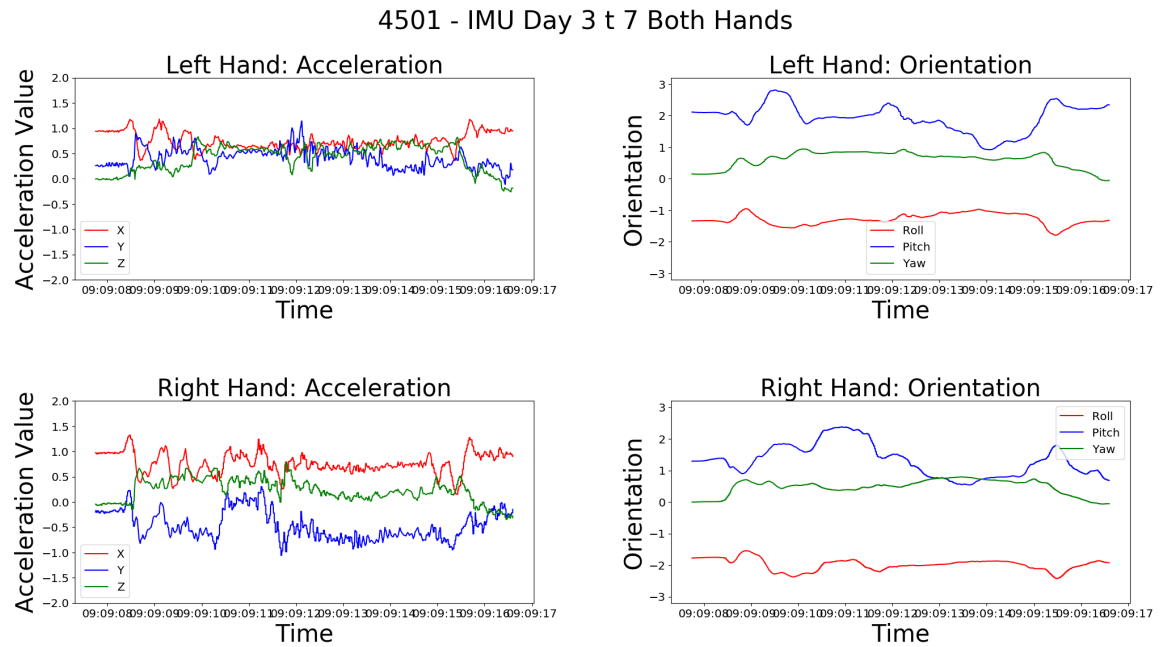


Figure 4.7.: IMU Data Plots for Acceleration and Orientation Data for Placing an IV Tourniquet

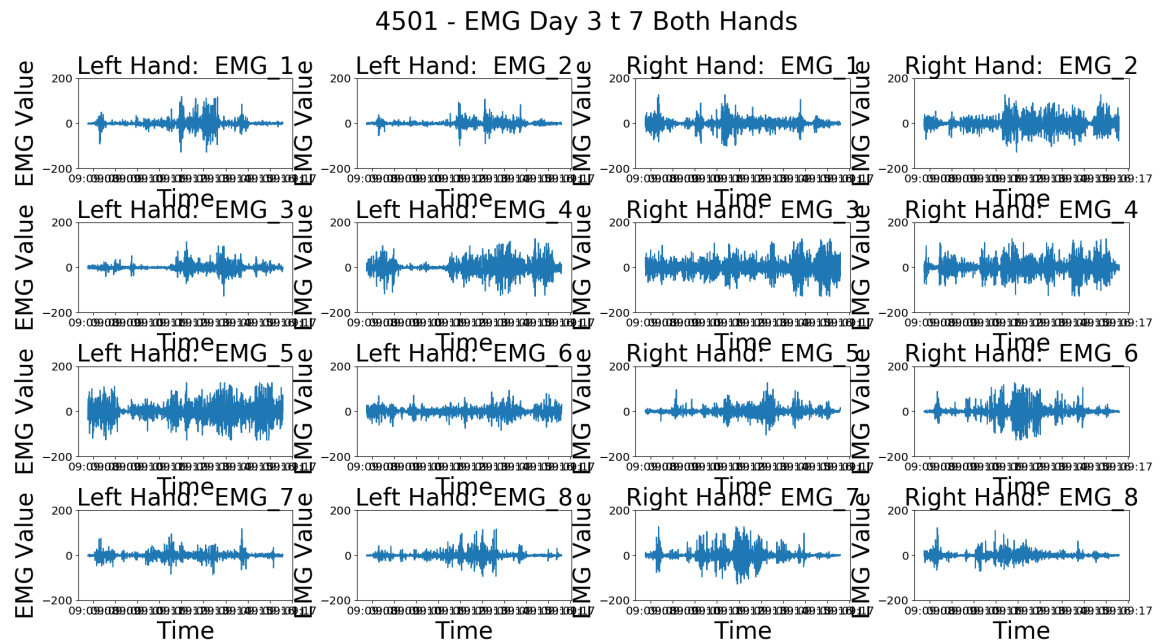


Figure 4.8.: EMG Data Plots for Placing an IV Tourniquet

substantial amount of activity related to the grabbing and releasing of the bandage when wrapping around the patient's head.

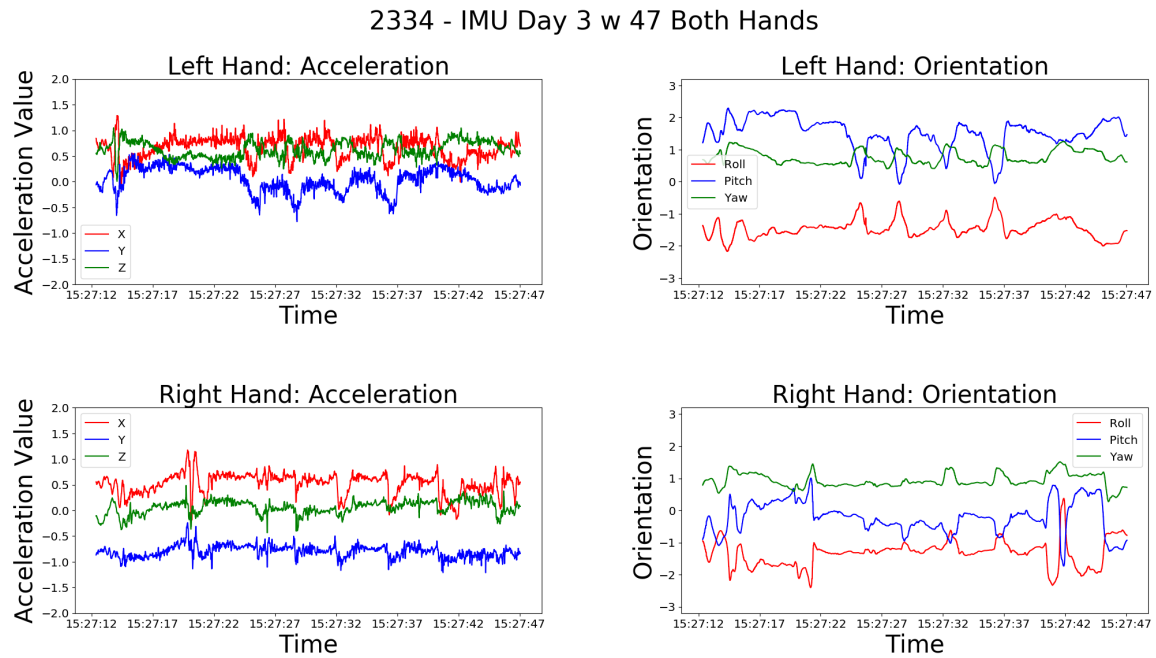


Figure 4.9.: IMU Data Plots for Acceleration and Orientation Data for wrapping a head wound

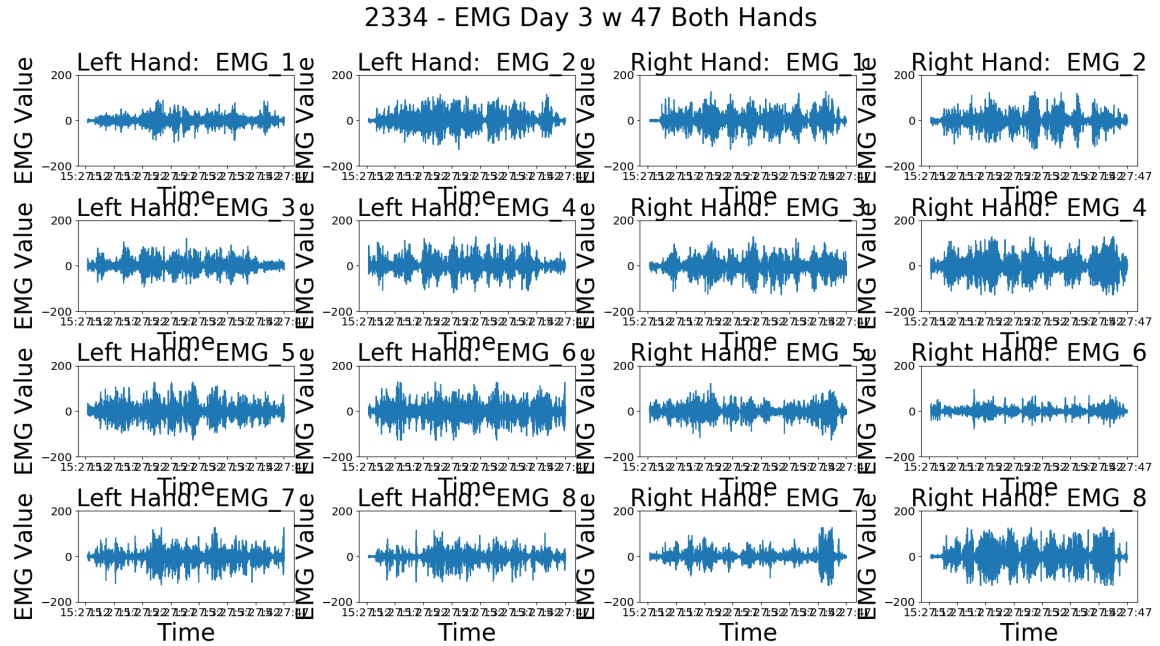


Figure 4.10.: EMG Data Plots for Wrapping a Head Wound

4.1.1. IMU and EMG Patterns Discussion

The average time it takes to complete a procedure was used to detect potential outliers. Participants average time had to be within the standard deviation to be considered for the

4. Results

combined dataset of participant generalizability. Participant's 5 average time was outside of the overall average for all procedures and removed for the combined dataset.

The sinusoidal movement of the chest compressions in the acceleration data when performing the CPR procedure can make it easy for a machine learning algorithm to pick up on, due to the unique value for the signal magnitude area feature. The sequence of applying chest compressions twice during one run of the procedure can help the HMM algorithm identify CPR better, because of similar values occurring multiple times.

The Bag-Valve-Mask ventilation procedure has a unique movement repeatedly squeezing the bag. The repetitive motion will be clearly represented in the signal magnitude area feature as well as the standard deviation feature for the EMG data.

Placing a IV tourniquet and an oral airway took participants the shortest time to complete. These short procedures can make it harder for a machine learning algorithm to identify the procedure, as only few window iterations will occur during the length of the procedure.

The repeated wrapping motion of bandaging a head wound can help machine learning algorithm identify the procedure. The movement is clearly visible in both acceleration and orientation data of the IMU.

The patterns identified above can improve detection accuracy through the generated features when training machine learning algorithms with the collected data. The signal magnitude area is able to pick up periodic movement, the mean is able to generate a baseline of motion, and the standard deviation depicts the quantity of motion.

4.2. Individual Participant Results

Each individual participant's datasets were used to train the decision-tree, SVM, k -NN, and HMM machine learning algorithms. The F1, precision, and recall scores by participant for the CPR procedure are provided in Table 4.1. The first participant had the lowest F1 score of all machine learning algorithms with 0.69 for the decision-tree, 0.31 for k -NN, 0.28 for SVM, 0.00 for HMM. The HMM varied the most across participants when recognizing CPR .

Bag-Valve-Mask ventilation achieved the lowest F1 scores of all procedures with F1 scores as low as 0.08, as seen in Table 4.2. The HMM classifier achieved the highest mean F1 score at 0.64 (Std. Dev=0.19), followed by the decision-tree algorithm at 0.60 (Std. Dev=0.09), and SVM algorithm at 0.26 (Std. Dev=0.06). The k -NN algorithm came last with a F1 score of 0.14 (Std. Dev=0.11).

Placing an oral airway was the most difficult procedure to detect, with F1 scores as low as 0.12, as seen in Table 4.3. The decision-tree classifier was the algorithm with the highest mean F1 score at 0.63 (Std. Dev=0.08), followed by the HMM algorithm at 0.51 (Std. Dev=0.27), and SVM algorithm at 0.20 (Std. Dev=0.04). The k -NN algorithm came last with a F1 score of 0.12 (Std. Dev=0.08).

Placing an IV tourniquet achieved a good F1 score for all machine learning algorithms except the HMM algorithm, as seen in Table 4.4. The decision-tree classifier was the algorithm with the highest mean F1 score at 0.81 (Std. Dev=0.06), followed by the SVM

Participant	decision-tree			<i>k</i> -NN (<i>k</i> = 4)			SVM			HMM		
	Precision	Recall	F1	Precision	Recall	F1	Precision	Recall	F1	Precision	Recall	F1
1	0.69	0.69	0.69	0.37	0.27	0.31	0.37	0.22	0.28	0.00	0.00	0.00
2	0.85	0.83	0.84	0.36	0.19	0.25	0.42	0.36	0.39	0.44	0.67	0.53
3	0.84	0.81	0.82	0.41	0.24	0.31	0.42	0.37	0.39	0.40	0.33	0.36
4	0.84	0.86	0.85	0.54	0.33	0.41	0.55	0.47	0.51	0.42	0.83	0.56
5	0.81	0.82	0.82	0.66	0.37	0.47	0.66	0.50	0.57	0.29	0.67	0.40
6	0.78	0.80	0.79	0.36	0.16	0.22	0.40	0.34	0.37	0.36	0.67	0.47
7	0.89	0.91	0.90	0.55	0.44	0.49	0.68	0.53	0.60	0.38	1.00	0.55
8	0.89	0.90	0.89	0.22	0.09	0.13	0.42	0.37	0.40	0.12	0.17	0.14
9	0.90	0.87	0.88	0.49	0.23	0.31	0.61	0.47	0.53	0.50	0.83	0.62
10	0.83	0.77	0.80	0.50	0.27	0.35	0.54	0.45	0.49	0.50	0.67	0.57
Mean	0.83	0.83	0.83	0.45	0.26	0.33	0.51	0.41	0.45	0.34	0.58	0.42
Std. Dev.	0.06	0.07	0.06	0.13	0.10	0.11	0.12	0.09	0.10	0.16	0.32	0.20

Table 4.1.: Ten-fold cross validation for detecting CPR per participant. Note: Bold represents the highest performance across a row

algorithm at 0.53 (Std. Dev=0.10), and *k*-NN at 0.40 (Std. Dev=0.05). The HMM algorithm came last with a F1 score of 0.24 (Std. Dev=0.21).

Wrapping a head wound achieved the highest F1 for the decision-tree algorithm, as seen in Table 4.5. The decision-tree classifier had a mean F1 score of 0.90 (Std. Dev=0.06), followed by the SVM algorithm at 0.61 (Std. Dev=0.04), and *k*-NN at 0.50 (Std. Dev=0.04). The HMM algorithm came last with a F1 score of 0.40 (Std. Dev=0.18)

4.2.1. Individual Participant Results Discussion

Contrary to the initial assumption in H_1 , recognition of CPR and Bag-valve-mask ventilation will have the highest accuracy for each machine learning algorithm, due to its unique movements, the unique movements during CPR were not as helpful to accurately detect the procedure. The hypothesis was not supported. The overlap of the giving breaths motion resulted in CPR being misclassified as Bag-Valve-Mask ventilation. Segmenting out the chest-compressions from the breathing motions and only training using the chest-compressions may result in higher accuracy due to the chest-compressions not appearing in any other procedure.

The Bag-Valve-Mask ventilation procedure has such a unique squeezing movement that the initial assumption concluded that it will be one of the easiest procedures to detect. In contrast it turned out to be one of the hardest, which may be due to its movement overlap with CPR.

The F1 scores show that detecting the placement of an oral airway is challenging. The short duration for the placemet does not leave much time for the algorithm to detect unique movements. The grabbing and spinning motion can occur in several other procedures when equipment are picked up and put into place.

4. Results

Participant	decision-tree			k -NN ($k = 4$)			SVM			HMM		
	Precision	Recall	F1	Precision	Recall	F1	Precision	Recall	F1	Precision	Recall	F1
1	0.81	0.48	0.60	0.67	0.30	0.41	0.31	0.19	0.23	0.50	0.25	0.33
2	0.79	0.78	0.78	0.58	0.17	0.27	0.31	0.23	0.26	0.90	0.75	0.82
3	0.56	0.54	0.55	0.32	0.13	0.18	0.32	0.26	0.29	0.88	0.70	0.78
4	0.47	0.45	0.46	0.27	0.06	0.10	0.22	0.20	0.21	0.71	0.50	0.59
5	0.71	0.58	0.64	0.11	0.04	0.05	0.24	0.25	0.25	0.86	0.60	0.71
6	0.55	0.50	0.53	0.33	0.07	0.12	0.38	0.29	0.32	0.60	0.33	0.43
7	0.62	0.63	0.63	0.28	0.07	0.12	0.26	0.24	0.25	1.00	0.57	0.73
8	0.50	0.52	0.51	0.18	0.05	0.08	0.16	0.14	0.15	0.57	0.44	0.50
9	0.63	0.59	0.61	0.33	0.09	0.14	0.33	0.35	0.34	0.80	0.44	0.57
10	0.67	0.63	0.65	0.12	0.02	0.03	0.30	0.33	0.32	1.00	0.90	0.95
Mean	0.63	0.57	0.60	0.31	0.10	0.14	0.28	0.25	0.26	0.78	0.55	0.64
Std. Dev.	0.12	0.01	0.09	0.17	0.08	0.11	0.07	0.06	0.06	0.18	0.20	0.19

Table 4.2.: Ten-fold cross validation for detecting BVM ventilation per participant

The low score of the HMM algorithm for placing an intravenous tourniquet can be a result of a close log probability of the HMM models. The HMM algorithm picks the highest log probability when data is tested on all HMM models. If the log probability are close it can mean the motion is easily interchangeable.

The HMM algorithm for wrapping a head wound under performed at detecting the procedure and had the highest standard deviation across participants. Participant seven achieved 0.92 for the decision-tree algorithm, but 0.00 for the HMM algorithm. The wide gap between recognition scores can contribute to the problem the HMM algorithm has with selecting the best model given the log probabilities.

4.3. Participant Generalizability

The datasets of all participants is combined to create one large dataset. The F1 score in Table 4.6 is lower when comparing the machine learning algorithms on the combined dataset to the individual participants, Tables 4.1 through 4.5. The highest F1 score on the combined dataset is achieved by the decision-tree algorithm with 0.71. The HMM algorithm followed second with 0.44, then k -NN with 0.35, and last the SVM with 0.25. Wrapping a wound (W) was the procedure with the highest F1 score for the decision-tree, k -NN ($k = 4$) and SVM algorithm. Bag-Valve-Mask ventilation (B) was the procedure with the highest F1 score for the HMM algorithm. The differences in movement between participants can be seen in Figure 4.11. The Figure shows the average of placing an intravenous tourniquet for all participants in red. Similarities between the average EMG data and the data of the participant can be seen, yet some noise is observable in channels three, four, and five.

Participant	decision-tree			<i>k</i> -NN (<i>k</i> = 4)			SVM			HMM		
	Precision	Recall	F1	Precision	Recall	F1	Precision	Recall	F1	Precision	Recall	F1
1	0.47	0.58	0.52	0.26	0.14	0.18	0.24	0.18	0.21	0.00	0.00	0.00
2	0.63	0.56	0.59	0.29	0.10	0.15	0.19	0.21	0.20	1.00	0.50	0.67
3	0.67	0.76	0.71	0.50	0.17	0.25	0.29	0.24	0.26	0.78	0.70	0.74
4	0.68	0.65	0.66	0.44	0.10	0.17	0.26	0.21	0.23	0.86	0.67	0.75
5	0.66	0.66	0.66	0.00	0.00	0.00	0.29	0.17	0.22	0.62	0.56	0.59
6	0.71	0.71	0.71	0.27	0.06	0.10	0.16	0.15	0.16	0.75	0.67	0.71
7	0.60	0.59	0.60	0.12	0.03	0.05	0.23	0.18	0.20	0.50	0.14	0.22
8	0.71	0.78	0.74	0.38	0.12	0.19	0.28	0.20	0.23	0.25	0.11	0.15
9	0.62	0.66	0.64	0.09	0.04	0.05	0.15	0.11	0.13	0.80	0.50	0.62
10	0.54	0.59	0.57	0.40	0.06	0.10	0.16	0.13	0.14	0.67	0.57	0.62
Mean	0.63	0.65	0.63	0.28	0.08	0.12	0.22	0.18	0.20	0.62	0.44	0.51
Std. Dev.	0.08	0.08	0.08	0.16	0.05	0.08	0.06	0.04	0.04	0.30	0.26	0.27

Table 4.3.: Ten-fold cross validation for detecting oral airway placement per participant

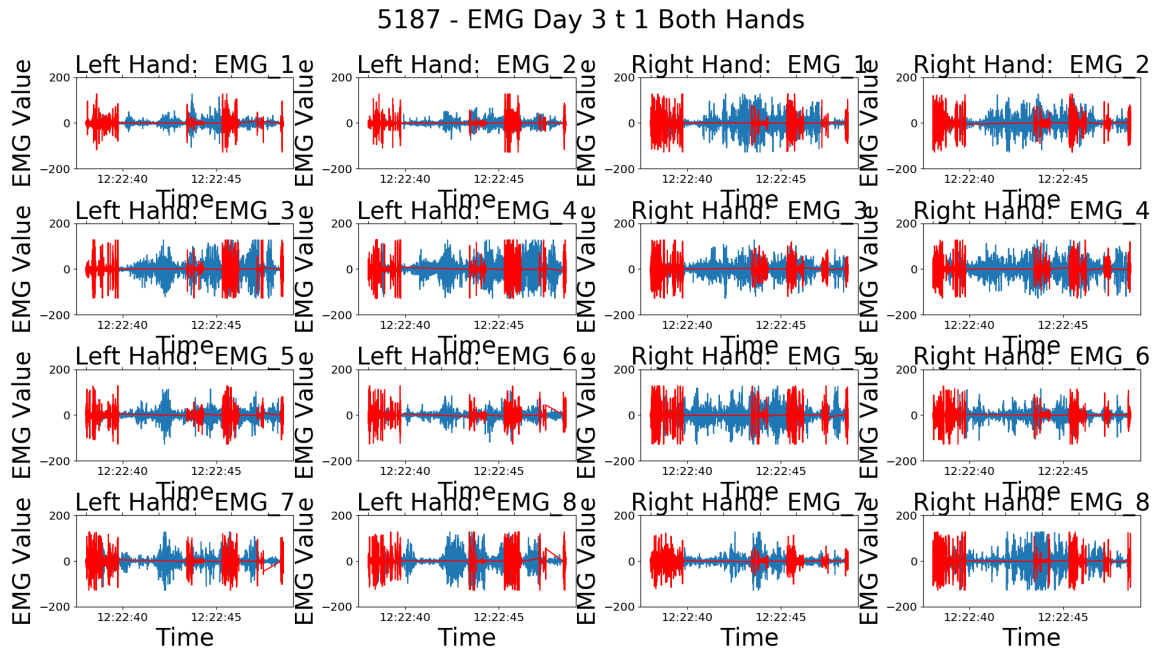


Figure 4.11.: Tourniquet EMG data with average in red

4.3.1. Participant Generalizability Discussion

The combined dataset allowed the machine learning algorithms to train on several participants, each participant with different approaches to the procedures. The unique movements may all look similar, but the way participants grab and adjust tools can be different. The F1 score for the generalized population is close to the results generated for individual participants. The F1 score of the decision-tree algorithm for tying a tourniquet was on

Participant	decision-tree			<i>k</i> -NN (<i>k</i> = 4)			SVM			HMM		
	Precision	Recall	F1	Precision	Recall	F1	Precision	Recall	F1	Precision	Recall	F1
1	0.65	0.65	0.65	0.30	0.36	0.33	0.29	0.30	0.30	0.22	0.40	0.29
2	0.80	0.81	0.80	0.31	0.56	0.40	0.51	0.62	0.56	0.00	0.00	0.00
3	0.83	0.81	0.82	0.30	0.57	0.39	0.43	0.56	0.49	0.00	0.00	0.00
4	0.84	0.85	0.84	0.37	0.64	0.47	0.56	0.67	0.61	0.50	0.17	0.25
5	0.85	0.87	0.86	0.34	0.64	0.45	0.54	0.71	0.61	0.00	0.00	0.00
6	0.83	0.80	0.82	0.31	0.42	0.36	0.48	0.59	0.53	0.33	0.17	0.22
7	0.80	0.79	0.80	0.27	0.44	0.33	0.42	0.55	0.48	0.22	0.33	0.27
8	0.89	0.86	0.87	0.33	0.60	0.43	0.50	0.66	0.57	0.60	0.50	0.55
9	0.80	0.78	0.79	0.34	0.53	0.41	0.47	0.59	0.53	0.75	0.50	0.60
10	0.80	0.84	0.82	0.28	0.52	0.37	0.43	0.53	0.58	0.25	0.17	0.20
Mean	0.81	0.81	0.81	0.32	0.52	0.40	0.46	0.60	0.53	0.30	0.22	0.24
Std. Dev.	0.06	0.06	0.06	0.03	0.10	0.05	0.08	0.11	0.10	0.26	0.20	0.21

Table 4.4.: Ten-fold cross validation for detecting tourniquet placement per participant

average 0.81 per participant and 0.74 across all participants. For wrapping a wound the F1 of the decision-tree algorithm was on average 0.90 per participant and 0.82 across all participants. Therefore, the algorithms are able to generalize across participants. The algorithms are also able to accurately detect a subset of procedures used inside an ambulance. While some procedures can be detected more accurately, others need improvements before the system can be deployed in real life scenarios.

4.4. Discussion

The results clearly show that it is feasible to successfully recognize procedures performed by EMS personnel on patients using the Myo sensor. The F1 score leaves room for improvement. The comparison between the decision-tree, *k*-NN, SVM, and HMM algorithm highlight the strengths of the decision-tree algorithm. The results also show a high variance in accuracy depending on the algorithm and procedure. The algorithms were able to successfully detect the procedures both individually and over all participants.

H_1 hypothesized that CPR and Bag-valve-mask ventilation will have the highest accuracy for each machine learning algorithm, due to its unique movements. CPR and Bag-valve-mask ventilation had neither the highest F1 score for individual participants or for all participants. The result shows that more data preparation needs to take place in order to separate similar movements, such as dividing the procedures further into their task and training the algorithms on a task basis, while using the sequence of tasks to detect the procedure.

H_2 hypothesized that the recognition of a procedure through the sequence of fine-grained movements using a Hidden Markov Model will be more accurate than detection through training coarse-grained movement models. The HMM algorithm achieved the

Participant	decision-tree			<i>k</i> -NN (<i>k</i> = 4)			SVM			HMM		
	Precision	Recall	F1	Precision	Recall	F1	Precision	Recall	F1	Precision	Recall	F1
1	0.73	0.72	0.72	0.43	0.54	0.48	0.47	0.66	0.55	0.20	0.20	0.20
2	0.88	0.91	0.89	0.45	0.46	0.46	0.60	0.58	0.59	0.30	0.50	0.37
3	0.81	0.83	0.82	0.42	0.42	0.42	0.63	0.62	0.62	0.38	0.83	0.53
4	0.91	0.90	0.90	0.43	0.49	0.46	0.61	0.63	0.62	0.22	0.33	0.27
5	0.87	0.87	0.87	0.42	0.39	0.40	0.63	0.63	0.63	0.29	0.33	0.31
6	0.88	0.90	0.89	0.45	0.65	0.53	0.54	0.55	0.55	0.44	0.67	0.53
7	0.92	0.91	0.92	0.49	0.54	0.51	0.60	0.65	0.62	0.00	0.00	0.00
8	0.94	0.92	0.93	0.43	0.48	0.45	0.62	0.59	0.61	0.25	0.50	0.33
9	0.88	0.90	0.89	0.49	0.55	0.51	0.68	0.68	0.68	0.45	0.83	0.59
10	0.92	0.93	0.93	0.44	0.51	0.47	0.66	0.67	0.67	0.38	0.50	0.43
Mean	0.90	0.90	0.90	0.44	0.50	0.50	0.60	0.63	0.61	0.30	0.50	0.40
Std. Dev.	0.06	0.06	0.06	0.03	0.07	0.04	0.06	0.04	0.04	0.13	0.30	0.18

Table 4.5.: Ten-fold cross validation for detecting wrapping a wound per participant

Procedure	decision-tree			<i>k</i> -NN (<i>k</i> = 4)			SVM			HMM		
	Precision	Recall	F1	Precision	Recall	F1	Precision	Recall	F1	Precision	Recall	F1
T	0.73	0.74	0.74	0.33	0.56	0.41	0.53	0.62	0.57	0.29	0.36	0.32
W	0.82	0.82	0.82	0.42	0.45	0.43	0.57	0.72	0.64	0.19	0.20	0.20
B	0.39	0.38	0.39	0.24	0.07	0.11	0.18	0.10	0.13	0.69	0.71	0.70
O	0.48	0.46	0.47	0.23	0.06	0.10	0.25	0.13	0.17	0.60	0.33	0.43
C	0.69	0.69	0.69	0.42	0.27	0.33	0.48	0.35	0.41	0.39	0.50	0.44
All	0.71	0.71	0.71	0.37	0.37	0.35	0.49	0.52	0.49	0.47	0.44	0.44

Table 4.6.: Ten-fold cross validation for all participants by procedure and algorithm. Note: T is intravenous tourniquet, W is wrapping a wound, B is Bag-Valve-Mask ventilation, O is oral airway, and C is CPR

highest F1 score for Bag-Valve-Mask ventilation with the individual participants results. The overall participant generalizability placed the HMM algorithm third.

The F1 score for the HMM was expected to be significantly higher given its ability to detect data sequences. The results from training using individual participants and all participants show that the HMM placed second behind the decision-tree.

The F1 score of the SVM was lower than expected. Missing computing power for the large dataset resulted in limited ability to vary the parameters to improve the accuracy.

The machine learning algorithms can be further improved by varying the parameters to a greater extent. The low performing SVM algorithm can be improved by varying the *gamma* and *C* value, and using a different kernel function.

4. Results

The Hidden Markov Model algorithm can be further improved by optimizing selection of winners for all the models. Currently, the model with highest the log probability is picked as the correct result. The function can be improved by re-running the data, if the log probability of two models are withing a certain margin of error or printing out the probabilities to let the EMS personnel confirm the performed procedure after they return to their base.

Additionally, the Hidden Markov Model can be trained in a supervised manner. The hierarchical task analysis provides detail about the states included in a procedure. The states can be pre-defined and transition probabilities inferred. Furthermore, deep-learning algorithms, such as neural networks may achieve higher scores in case nonlinearity occurs in the dataset.

The generalizability can be further improved by collecting data from more participants. The data used in this thesis required participants to use specific hands for every procedure. Data, which includes left- and right-handed participants increases the generalizability.

The procedures represent those performed by EMS personnel on the way to the hospital inside of an ambulance. The movement of the ambulance introduces noise that can effect the accuracy of the machine learning algorithms. Future work can collect data in an ambulance simulation to improve real-life application.

Ambulances may include multiple EMS personnel, who can work on the patient simultaneously. The sensor has to be placed on all EMS personnel working on the patient in order to correctly identify the procedure. Future work can collect data from multiple participants at the same time and improve the machine learning algorithm to include data from more than two sensors.

Lastly, data from professionally trained EMS personnel may result in more consistent data, which may improve the score of all machine learning algorithms.

Overall, in order to use the technology in real world application, such as transmitting treatment information to a hospital in real-time requires a significantly higher detection accuracy. Unreliable treatment information can result in wrong preparation at the hospital, which may cause permanent injury or result in death. The procedure detection system needs to be further evaluated in real-life non-life threatening scenarios in order to obtain its effectiveness in improving communication between EMS personnel and hospital trauma staff. While there is room for improvement, the thesis is an initial step in detecting procedures inside of an ambulance.

5. Conclusion

This thesis provided a novel approach to recognize CPR, bag-valve-mask ventilation, placing an oral airway, placing an IV tourniquet, and wrapping a head wound using data collected by the Myo and machine-learning algorithms. The five procedures were broken into their anatomical movements using hierarchical task analysis. The Myo sensor was chosen for its ability to sense most of the anatomical movements. Data from the Myo was processed and seven features were generated. The SVM, k -NN, and decision-tree machine learning algorithms were compared to Hidden Markov Models for every procedure. A user evaluation with ten participants was used to obtain the data necessary to train and evaluate the algorithms. The participants were trained in the procedures for two days, and data was collected on the third day. The Decision-tree achieved the highest F1 score and is feasible for inclusion into a system that automatically detects EMS procedures. The machine learning algorithms were applied to data from every individual participant and compared to data from all participants combined. The F1 score for the procedures were similar within a small margin and the data can therefore be considered generalizable.

Future work will be able to further segment the procedures to limit the detection to a specific task rather than the entire procedure. Through the series of tasks the procedure can then be implied. The use of artificial neural networks may also improve the detection accuracy and yield better results at detecting the subset of procedures. When higher detection results are achieved more procedures can be included in the detection system.

The EMS procedure detection system can already use the developed algorithms to assist EMS personnel in filling out paperwork by suggesting the detected procedure. The procedure detection system allows for faster paper work completion without any harm for the treatment of the patient.

Bibliography

- [1] Atiqur Rahman Ahad, Tetsuya Ogata, Joo Kooi Tan, Hyoungseop Kim, and Seiji Ishikawa. "Motion recognition approach to solve overwriting in complex actions". In: *IEEE International Conference on Automatic Face Gesture Recognition*. Sept. 2008, pp. 1–6.
- [2] Norhafizan Ahmad, Raja Ariffin Raja Ghazilla, Nazirah M. Khairi, and Vijayabaskar Kasi. "Reviews on Various Inertial Measurement Unit (IMU) Sensor Applications". In: *International Journal of Signal Processing Systems* 1.2 (2013), pp. 256–262.
- [3] Muhammad Arif and Ahmed Kattan. "Physical Activities Monitoring Using Wearable Acceleration Sensors Attached to the Body". In: *PLOS ONE* 10.7 (July 2015), pp. 1–16.
- [4] Katrin Arning and Martina Ziefle. "“Get that Camera Out of My House!” Conjoint Measurement of Preferences for Video-Based Healthcare Monitoring Systems in Private and Public Places". In: *Inclusive Smart Cities and e-Health*. Ed. by Antoine Geissbühler, Jacques Demongeot, Mounir Mokhtari, Bessam Abdulrazak, and Hamdi Aloulou. Cham: Springer International Publishing, 2015, pp. 152–164.
- [5] Vineet Arora and Julie Johnson. "A model for building a standardized hand-off protocol". In: *Joint Commission Journal on Quality and Patient Safety* 32.11 (2006), pp. 646–655.
- [6] Leonard E. Baum, Ted Petrie, George Soules, and Norman Weiss. "A Maximization Technique Occurring in the Statistical Analysis of Probabilistic Functions of Markov Chains". In: *Ann. Math. Statist.* 41.1 (Feb. 1970), pp. 164–171.
- [7] Marco E Benalcázar, Andrés G Jaramillo, A Zea, and Andrés Páez. "Hand Gesture Recognition Using Machine Learning and the Myo Armband". In: *European Signal Processing Conference* (2017), pp. 1075–1079.
- [8] J. R. Beveridge, P. J. Phillips, D. S. Bolme, B. A. Draper, G. H. Givens, Y. M. Lui, M. N. Teli, H. Zhang, W. T. Scruggs, K. W. Bowyer, P. J. Flynn, and S. Cheng. "The challenge of face recognition from digital point-and-shoot cameras". In: *IEEE International Conference on Biometrics: Theory, Applications and Systems*. Sept. 2013, pp. 1–8.
- [9] Gevdeep Bhabra, Samuel Mackeith, Pedro Monteiro, and David D. Pothier. "An experimental comparison of handover methods". In: *Annals of the Royal College of Surgeons of England* 89.3 (2007), pp. 298–300.
- [10] F. Bianchi, S. J. Redmond, M. R. Narayanan, S. Cerutti, and N. H. Lovell. "Barometric Pressure and Triaxial Accelerometry-Based Falls Event Detection". In: *IEEE Transactions on Neural Systems and Rehabilitation Engineering* 18.6 (Dec. 2010), pp. 619–627.

Bibliography

- [11] Aaron F. Bobick and James W. Davis. "The Recognition of Human Movement Using Temporal Templates". In: *IEEE Transactions on Pattern Analysis & Machine Intelligence* 23 (Mar. 2001), pp. 257–267.
- [12] Agata Brajdic and Robert Harle. "Walk Detection and Step Counting on Unconstrained Smartphones". In: *ACM International Joint Conference on Pervasive and Ubiquitous Computing*. UbiComp '13. Zurich, Switzerland: ACM, 2013, pp. 225–234.
- [13] Bhaskar Chakraborty, Ognjen Rudovic, and Jordi Gonzàlez. "View-invariant human-body detection with extension to human action recognition using component-wise HMM of body parts". In: *IEEE International Conference on Automatic Face and Gesture Recognition* (2008), pp. 1–6.
- [14] Faicel Chamroukhi, Samer Mohammed, Dorra Trabelsi, Latifa Oukhellou, and Yacine Amirat. "Joint segmentation of multivariate time series with hidden process regression for human activity recognition". In: 120 (Dec. 2013).
- [15] Hsuan-Sheng Chen, Hua-Tsung Chen, Yi-Wen Chen, and Suh-Yin Lee. "Human Action Recognition Using Star Skeleton". In: *ACM International Workshop on Video Surveillance and Sensor Networks*. Santa Barbara, California, USA: ACM, 2006, pp. 171–178.
- [16] L. Cheng, Y. Guan, Kecheng Zhu, and Yiyang Li. "Recognition of human activities using machine learning methods with wearable sensors". In: *IEEE Annual Computing and Communication Workshop and Conference*. Jan. 2017, pp. 1–7.
- [17] Michael D. Cohen and P. Brian Hilligoss. "The published literature on handoffs in hospitals: Deficiencies identified in an extensive review". In: *Quality and Safety in Health Care* 19.6 (2010), pp. 493–497.
- [18] Sarah A. Collins, Daniel M. Stein, David K. Vawdrey, Peter D. Stetson, and Suzanne Bakken. "Content overlap in nurse and physician handoff artifacts and the potential role of electronic health records: A systematic review". In: *Journal of Biomedical Informatics* 44.4 (2011), pp. 704–712.
- [19] 104th Congress. *Health Insurance Portability and Accountability Act*. Pub.L. 104–191. 1996.
- [20] CRICO Strategies. *Malpractice Risks in Communication Failures 2015 Annual Benchmarking Report*. Tech. rep. Boston, MA: The Risk Management Foundation of the Harvard Medical Institutions Incorporated, 2015, p. 24.
- [21] Carlo De Luca, L Donald Gilmore, Mikhail Kuznetsov, and Serge Roy. "Filtering the surface EMG signal: Movement artifact and baseline noise contamination". In: 43 (Mar. 2010), pp. 1573–9.
- [22] David Doermann, Jian Liang, and Huiping Li. "Progress in camera-based document image analysis". In: *Document Analysis and Recognition, 2003. Proceedings. Seventh International Conference on*. IEEE. 2003, pp. 606–616.
- [23] Alexei A. Efros, Alexander C. Berg, Greg Mori, and Jitendra Malik. "Recognizing Action at a Distance". In: *IEEE International Conference on Computer Vision*. Nice, France, 2003, pp. 726–733.

- [24] Kris van Erum and Johannes Schöning. “SubwayAPPS: Using Smartphone Barometers for Positioning in Underground Transportation Environments”. In: *Progress in Location-Based Services 2016*. Springer, 2017, pp. 69–85.
- [25] David A. Forsyth, Okan Arikan, Leslie Ikemoto, James O’Brien, and Deva Ramanan. “Computational Studies of Human Motion: Part 1, Tracking and Motion Synthesis”. In: *Foundations and Trends in Computer Graphics and Vision* 1.2–3 (2006), pp. 77–254.
- [26] Dirk Gehrig, Peter Krauthausen, Lukas Rybok, Hildegard Kühne, Tanja Schultz, Uwe D Hanebeck, and Rainer Stiefelhagen. “Combined Multi-Level Intention, Activity, and Motion Recognition for a Humanoid Robot (preliminary)”. In: *Proceedings of the IEEE/RSJ International Conference on Intelligent Robots and Systems* (2011), pp. 4819–4825.
- [27] Dirk Gehrig, Thorsten Stein, Andreas Fischer, Hermann Schwameder, and Tanja Schultz. “Towards Semantic Segmentation of Human Motion Sequences”. In: *Advances in Artificial Intelligence*. Ed. by Rüdiger Dillmann, Jürgen Beyerer, Uwe D. Hanebeck, and Tanja Schultz. Berlin, Heidelberg: Springer Berlin Heidelberg, 2010, pp. 436–443.
- [28] Hidalgo Gines, Cao Zhe, Simon Tomas, Wei Shih-En, Joo Hanbyul, and Yaser Sheikh. *OpenPose: Real-time multi-person keypoint detection library for body, face, and hands estimation*. <https://github.com/CMU-Perceptual-Lab/openpose>. Accessed on 03/02/2018. 2017–2018.
- [29] Nihal Fatma Güler and Sabri Koçer. “Classification of EMG Signals Using PCA and FFT”. In: *Journal of Medical Systems* 29.3 (June 2005), pp. 241–250.
- [30] Sumi Helal, Eunju Kim, and Diane Cook. “Human Activity Recognition and Pattern Discovery”. In: *IEEE Pervasive Computing* 9 (Jan. 2010), pp. 48–53.
- [31] Samitha Herath, Mehrtash Harandi, and Fatih Porikli. “Going deeper into action recognition: A survey”. In: *Image and Vision Computing* 60 (2017), pp. 4–21. eprint: 1605.04988.
- [32] Bernhard Hofmann-Wellenhof, Herbert Lichtenegger, and James Collins. *Global positioning system: theory and practice*. Springer Science & Business Media, 2012.
- [33] Nicholas R Howe, Michael E Leventon, and William T Freeman. “Bayesian reconstruction of 3d human motion from single-camera video”. In: *Advances in neural information processing systems*. 2000, pp. 820–826.
- [34] Stephanie Jeran, A Steinbrecher, and T Pischnon. “Prediction of activity-related energy expenditure using accelerometer-derived physical activity under free-living conditions: A systematic review”. In: (Feb. 2016).
- [35] Kanithika Kaewkannate and Soochan Kim. “A comparison of wearable fitness devices”. In: *BMC Public Health* 16.1 (May 2016), p. 433.
- [36] L.A.C. Kallenberg and H.J. Hermens. “Behaviour of a surface EMG based measure for motor control: Motor unit action potential rate in relation to force and muscle fatigue”. In: *Journal of Electromyography and Kinesiology* 18.5 (2008), pp. 780–788.

Bibliography

- [37] E. Kim, S. Helal, and D. Cook. “Human Activity Recognition and Pattern Discovery”. In: *IEEE Pervasive Computing* 9.1 (Jan. 2010), pp. 48–53.
- [38] Barry Kirwan and Les K. Ainsworth. *A Guide To Task Analysis: The Task Analysis Working Group*. A Guide to Task Analysis. Taylor & Francis, 1992.
- [39] B. Knorr, R. Hughes, D. Sherrill, J. Stein, M. Akay, and P. Bonato. “Quantitative Measures of Functional Upper Limb Movement in Persons after Stroke”. In: *Conference Proceedings. 2nd International IEEE EMBS Conference on Neural Engineering, 2005*. Mar. 2005, pp. 252–255.
- [40] Qin Kuang, Changshi Lao, Zhong Lin Wang, Zhaoxiong Xie, and Lansun Zheng. “High-Sensitivity Humidity Sensor Based on a Single SnO₂ Nanowire”. In: *Journal of the American Chemical Society* 129.19 (2007), pp. 6070–6071.
- [41] Hilde Kuehne, Hueihan Jhuang, Estibaliz Garrote, Tomaso A. Poggio, and Thomas Serre. “HMDB: A large video database for human motion recognition”. In: *Proceedings of the International Conference on Computer Vision*. 2011, pp. 571–582.
- [42] N. D. Lane, E. Miluzzo, H. Lu, D. Peebles, T. Choudhury, and A. T. Campbell. “A survey of mobile phone sensing”. In: *IEEE Communications Magazine* 48.9 (Sept. 2010), pp. 140–150.
- [43] Oscar D. Lara and Miguel A. Labrador. “A Survey on Human Activity Recognition using Wearable Sensors”. In: *IEEE Communications Surveys & Tutorials* 15.3 (2013), pp. 1192–1209.
- [44] Óscar D. Lara, Alfredo J. Prez, Miguel A. Labrador, and Jos D. Posada. “Centinela: A human activity recognition system based on acceleration and vital sign data”. In: *Pervasive and Mobile Computing* 8.5 (2012), pp. 717–729.
- [45] Y. LeCun, Fu Jie Huang, and L. Bottou. “Learning methods for generic object recognition with invariance to pose and lighting”. In: *IEEE Computer Society Conference on Computer Vision and Pattern Recognition*. Vol. 2. June 2004, pp. 97–104.
- [46] Lin Liao, Dieter Fox, and Henry Kautz. “Location-based activity recognition”. In: *Advances in Neural Information Processing Systems*. 2006, pp. 787–794.
- [47] A. J. Lipton, H. Fujiyoshi, and R. S. Patil. “Moving target classification and tracking from real-time video”. In: *Applications of Computer Vision, 1998. WACV '98. Proceedings., Fourth IEEE Workshop on*. Oct. 1998, pp. 8–14.
- [48] Marco Maier and Florian Dorfmeister. “Fine-Grained Activity Recognition of Pedestrians Travelling by Subway”. In: *Mobile Computing, Applications, and Services*. Ed. by Gérard Memmi and Ulf Blanke. Cham: Springer International Publishing, 2014, pp. 122–139.
- [49] U. Maurer, A. Smailagic, D.P. Siewiorek, and M. Deisher. “Activity Recognition and Monitoring Using Multiple Sensors on Different Body Positions”. In: *International Workshop on Wearable and Implantable Body Sensor Networks* (2006), pp. 113–116.

- [50] Zachary F. Meisel, Judy A. Shea, Nicholas J. Peacock, Edward T. Dickinson, Breah Paciotti, Roma Bhatia, Egor Buharin, and Carolyn C. Cannuscio. “Optimizing the patient handoff between emergency medical services and the emergency department”. In: *Annals of Emergency Medicine* 65.3 (2015), 310–317.e1.
- [51] Quentin Mourcou, Anthony Fleury, Céline Franco, Frédéric Klopcic, and Nicolas Vuillerme. “Performance evaluation of smartphone inertial sensors measurement for range of motion”. In: *Sensors* 15.9 (2015), pp. 23168–23187.
- [52] Sarfraz Nawaz, Christos Efstratiou, and Cecilia Mascolo. “ParkSense: A Smartphone Based Sensing System for On-street Parking”. In: *Proceedings of the 19th Annual International Conference on Mobile Computing & Networking*. MobiCom ’13. Miami, Florida, USA: ACM, 2013, pp. 75–86.
- [53] J. Nishimura and T. Kuroda. “Multiaxial Haar-Like Feature and Compact Cascaded Classifier for Versatile Recognition”. In: *IEEE Sensors Journal* 10.11 (Nov. 2010), pp. 1786–1795.
- [54] Abhinav Parate, Meng-Chieh Chiu, Chaniel Chadowitz, Deepak Ganesan, and Evangelos Kalogerakis. “RisQ: Recognizing Smoking Gestures with Inertial Sensors on a Wristband.” In: *MobiSys ... : the ... International Conference on Mobile Systems, Applications and Services. International Conference on Mobile Systems, Applications, and Services 2014* (2014), pp. 149–161. eprint: 15334406.
- [55] Juha Pärkkä, Miikka Ermes, Panu Korpijää, Jani Mäntyjärvi, Johannes Peltola, and Ilkka Korhonen. “Activity Classification Using Realistic Data From Wearable Sensors”. In: *IEEE Transactions on Information Technology in Biomedicine* 10 (Feb. 2006), pp. 119–28.
- [56] Ronald Poppe. “A survey on vision-based human action recognition”. In: *Image and Vision Computing* 28.6 (2010), pp. 976–990.
- [57] Mohammed A. Quddus, Washington Yotto Ochieng, Lin Zhao, and Robert B. Noland. “A general map matching algorithm for transport telematics applications”. In: *GPS Solutions* 7.3 (Dec. 2003), pp. 157–167.
- [58] Mary M. Rodgers, Vinay M. Pai, and Richard S. Conroy. “Recent advances in wearable sensors for health monitoring”. In: *IEEE Sensors Journal* 15.6 (2015), pp. 3119–3126.
- [59] Oliver C Schrempf and Uwe D Hanebeck. “A Generic Model for Estimating User Intentions in Human-Robot Cooperation”. In: *Proceedings of the International Conference on Informatics in Control, Automation and Robotics* (2005), pp. 251–256.
- [60] Sheng Shen, He Wang, and Romit Roy Choudhury. “I Am a Smartwatch and I Can Track My User’s Arm”. In: *Proceedings of the 14th Annual International Conference on Mobile Systems, Applications, and Services*. MobiSys ’16. Singapore, Singapore: ACM, 2016, pp. 85–96.
- [61] John Ortiz Smykla, Matthew S. Crow, Vaughn J. Crichlow, and Jamie A. Snyder. “Police Body-Worn Cameras: Perceptions of Law Enforcement Leadership”. In: *American Journal of Criminal Justice* 41.3 (2016), pp. 424–443.

Bibliography

- [62] Darrell J. Solet, J. Michael Norvell, Gale H. Rutan, and Richard M. Frankel. “Lost in translation: challenges and opportunities in physician to physician communication during patient handoff.” In: *Academic Medicine* 80.12 (2005), pp. 1094–1099.
- [63] Rosemary Spencer, Enrico Coiera, and Pamela Logan. “Variation in communication loads on clinical staff in the emergency department”. In: *Annals of Emergency Medicine* 44.3 (2004), pp. 268–273.
- [64] Amy J. Starmer, Nancy D. Spector, Rajendu Srivastava, Daniel C. West, Glenn Rosenbluth, April D. Allen, Elizabeth L. Noble, Lisa L. Tse, Anuj K. Dalal, Carol A. Keohane, Stuart R. Lipsitz, Jeffrey M. Rothschild, Matthew F. Wien, Catherine S. Yoon, Katherine R. Zigmont, Karen M. Wilson, Jennifer K. O’Toole, Lauren G. Solan, Megan Aylor, Zia Bismilla, Maitreya Coffey, Sanjay Mahant, Rebecca L. Blankenburg, Lauren A. Destino, Jennifer L. Everhart, Shilpa J. Patel, James F. Jr. Bale, Jaime B. Spackman, Adam T. Stevenson, Sharon Calaman, F. Sessions Cole, Dorene F. Balmer, Jennifer H. Hepps, Joseph O. Lopreiato, Clifton E. Yu, Theodore C. Sectish, and Christopher P. Landrigan. “Changes in Medical Errors after Implementation of a Handoff Program”. In: *New England Journal of Medicine* 371.19 (2014), pp. 1803–1812.
- [65] Deutsches Strafgesetzbuch. §203 *Verletzung von Privatgeheimnissen*. 2017.
- [66] Michael S. Totty and Eric Wade. “Muscle Activation and Inertial Motion Data for Non-Invasive Classification of Activities of Daily Living”. In: *IEEE Transactions on Biomedical Engineering* 9294.c (2017), pp. 1–1.
- [67] TRUSTe/NCSA. *U.S. Consumer Privacy Index 2016*. <https://www.trustarc.com/resources/privacy-research/ncsa-consumer-privacy-index-us/>. Accessed on 03/02/2018. 2016.
- [68] Gitendra Uswatte and Laura Qadri. “A Behavioral Observation System for Quantifying Arm Activity in Daily Life After Stroke”. In: *Rehabilitation psychology* (Nov. 2009), pp. 398–403.
- [69] Johan Wannenburgh and Reza Malekian. “Physical Activity Recognition From Smartphone Accelerometer Data for User Context Awareness Sensing”. In: *IEEE Transactions on Systems, Man, and Cybernetics: Systems* 47.12 (2016), pp. 1–8.
- [70] Daniel Weinland, Remi Ronfard, and Edmond Boyer. “Free viewpoint action recognition using motion history volumes”. In: *Computer Vision and Image Understanding* 104 (2006), pp. 249–257.
- [71] T. Yang, W. Huang, C. K. Chui, Z. Jiang, and L. Jiang. “Stacked hidden Markov model for motion intention recognition”. In: *IEEE International Conference on Signal and Image Processing*. Aug. 2017, pp. 266–271.
- [72] Jie Yin, Qiang Yang, and Jeffrey Junfeng Pan. “Sensor-Based Abnormal Human-Activity Detection”. In: *IEEE Transactions on Knowledge and Data Engineering* 20.8 (Aug. 2008), pp. 1082–1090.
- [73] Mi Zhang and Alexander A. Sawchuk. “Human daily activity recognition with sparse representation using wearable sensors”. In: *IEEE Journal of Biomedical and Health Informatics* 17.3 (2013), pp. 553–560.

- [74] Yu Zheng, Like Liu, Longhao Wang, and Xing Xie. “Learning transportation mode from raw gps data for geographic applications on the web”. In: *Proceeding of the International Conference on World Wide Web* (2008), p. 247.

A. Appendix

Table A.1.: Hierarchical Task Analysis: CPR

Task	Sub-Sub-Tasks(If Applicable)	Task Movements	Devices					
			Apple Watch	MYO	Empatic E4	Garmin Watch Forerunner	Bioharness BT	Sensed?
1. CPR								
1.1. Lift Patient's Chin Multi-Hand Task		1.1.1. Move Hand onto Patient's Forehead 1.1.2. Move other Hand under Patient's Chin 1.1.3. Use Two Fingers to Lift Patient's Head past Neutral Position	L R R	✓ ✓ ✓	L R R	L R R	- - -	✓ ✓ ✓
1.2. Check for Breathing		1.2.1. Flex Torso and Turn Head such that your Ear is Next to the Patient's Mouth 1.2.2. Listen for Breaths 1.2.3. Unflex Torso and Turn Head	- - -	- - -	- - -	- - -	✓ - ✓	✓ - ✓
1.3A. Give 2 Breaths: No Mask Multi-Hand Task	1.3A.1. Pinch Patient's Nose	1.3A.1.1. Move Hand to Patient's Nose 1.3A.1.2. Close Thumb and Fingers to Pinch Patient's Nose	L -	✓ ✓	L	L	- -	✓ ✓
	1.3A.2. Give Breaths	1.3A.2.1. Flex Torso to Lean Over Patient 1.3A.2.2. Put Mouth over Patient's Mouth to make a Complete Seal 1.3A.2.3. Give Rescue Breath for 1 Second 1.3A.2.4. Wait 1 Second 1.3A.2.5. Give Rescue Breath for 1 Second 1.3A.2.6. Unflex Torso 1.3A.2.7. Open Thumb and Fingers to Unpinch Patient's Nose	- - - - - - -	- - - - - - -	- - - - - - -	- - - - - - -	✓ - ✓ - ✓ ✓ ✓	✓ - ✓ - ✓ ✓ ✓
1.3B. Give 2 Breaths: Valve Mask Multi-Hand Task	1.3B.1 Grab Valve Mask	1.3B.1.1. Move Arm to Valve Mask Storage Area 1.3B.1.2. Close Hand 1.3B.1.3. Move Arm to Patient's Head	L - L	✓ ✓ ✓	L	L	- - -	✓ ✓ ✓
	1.3B.2. Move Valve Mask into Position	1.3B.2.1. Move Arm Down to Place Mask Over the Patient's Mouth 1.3B.2.2. Place One Hand on Mask 1.3B.2.3. Use the Other Hand to Grab the Bag	L L R	✓ ✓ ✓	L L R	L L R	- - -	✓ ✓ ✓
	1.3B.3. Squeeze Bag Twice	1.3B.3.1. Close the Hand on the Bag for 1 Second 1.3B.3.2. Open the Hand 1.3B.3.3. Wait 4 Seconds 1.3B.3.4. Close the Hand on the Bag for 1 Second 1.3B.3.5. Open the Hand	- - - - -	✓ ✓ - ✓ ✓	- - - - -	- - - - -	- - - - -	✓ ✓ - ✓ ✓
	1.3B.4. Place Valve Mask in a Secure Location	1.3B.4.1. Take Hand off of the Mask 1.3B.4.2. Move Arm to Secure Location 1.3B.4.3. Open the Hand	L R -	✓ ✓ ✓	L R -	L R -	- - -	✓ ✓ ✓
1.4. Start Compressions Multi-Hand Task		1.4.1. Place One Hand on the Patient's Chest 1.4.2. Place the Other Hand on top of the Hand 1.4.3. Interlace Fingers 1.4.4. Position Shoulders so that they are Directly over your Hands 1.4.5. Lock Elbows 1.4.6. Use Upper Body Weight to Push Down on the Chest at 100-120 BPM 1.4.7. After 30 Compressions, Give 2 Breaths	L R - - - - L -	✓ ✓ - - - - ✓ -	L R - - - - L -	L R - - - - L -	- - - - - - - -	✓ ✓ - - - - ✓ -

Table A.2.: Hierarchical Task Analysis: Bag-Valve-Mask Ventilation

Task	Sub-Sub-Tasks(If Applicable)	Task Movements	Devices					
			Apple Watch	MYO	Empatic E4	Garmin Watch Forerunner	Bioharness BT	Sensed?
2. Bag-valve-mask ventilation								
2.1 Raise patient		2.1.1 Grab height lever of stretcher 2.1.2 Grab headrest handles of gurney with both hands 2.1.3 Pull up until patients ear is level with the sternal notch	- - L/R	✓ ✓ ✓	- - L/R	- - L/R	- - -	✓ ✓ ✓
2.2 Lift Patient's Chin Multi-hand Task		2.2.1. Move Hand onto Patient's Forehead 2.2.2. Move other Hand under Patient's Chin 2.2.3. Use Two Fingers to Lift Patient's Head past Neutral Position	L R -	✓ ✓ ✓	L R -	L R -	- - -	✓ ✓ ✓
2.3A Place oral airway (unresponsive)		2.3A.1 Place thumb on bottom teeth and index finger on upper teeth 2.3A.2 Move fingers outward to open mouth 2.3A.3 Insert airway upside down until it reaches back of tongue 2.3A.4 Rotate wrist 180 degrees	- - L/R L/R	✓ ✓ ✓ ✓	- - L/R L/R	- - L/R L/R	- - - -	✓ ✓ ✓ ✓
2.3B Place nasal airway (responsive)		2.3B.1 Pinch ends of tube with thumb and index finger 2.3B.2 Hold tube from nose to earlobe to measure length 2.3B.3 Rip open lubricant package by pulling the top in opposite directions 2.3B.2 Squeeze with thumb and index finger on the package to lubricate the tube 2.3B.3 Raise end of patients nose 2.3B.4 Insert tube into patients nostril with thumb and index finger	- L/R L/R - - L/R	✓ ✓ ✓ ✓ ✓ ✓	- L/R L/R - - L/R	- L/R L/R - - L/R	- - - - - -	✓ ✓ ✓ ✓ ✓ ✓
2.4 Ventilate the Patient Multi-hand Task	2.4.1 Grab Valve Mask	2.4.1.1. Move Arm to Valve Mask Storage Area 2.4.1.2. Close Hand 2.4.1.3. Move Arm to Patient's Head	L/R - L/R	✓ ✓ ✓	L/R - L/R	L/R - L/R	- - -	✓ ✓ ✓
	2.4.2. Move Valve Mask into Position	2.4.2.1. Move Arm Down to Place Mask Over the Patient's Mouth 2.4.2.2. Place One Hand on Mask 2.4.2.3. Use the Other Hand to Grab the Bag	L/R L R	✓ ✓ ✓	L/R L R	L/R L R	- - -	✓ ✓ ✓
	2.4.3. Repeat squeezing until patient has recovered	2.4.3.1. Close the Hand on the Bag for 1 Second 2.4.3.2. Open the Hand 2.4.3.3. Wait 4 Seconds 2.4.3.4. Close the Hand on the Bag for 1 Second 2.4.3.5. Open the Hand	- - - - -	✓ ✓ - ✓ ✓	- - - - -	- - - - -	- - - - -	✓ ✓ - ✓ ✓

Table A.3.: Hierarchical Task Analysis: Placing an Oral Airway

Task	Sub-Sub-Tasks (If Applicable)	Task Movements	Devices					
			Wearable					
3. Oral Airway			Apple Watch	MYO	Empatic E4	Garmin Watch Forerunner	Bioharness BT	Sensed?
3.1 Raise patient		3.1.1 Grab height lever of stretcher 3.1.2 Grab headrest handles of gurney with both hands 3.1.3 Pull up until patients ear is level with the sternal notch	- - L/R	✓ ✓ ✓	- - L/R	- - L/R	- - -	✓ ✓ ✓
3.2 Lift Patient's Chin Multi-Hand Task		3.2.1. Move Hand onto Patient's Forehead 3.2.2. Move other Hand under Patient's Chin 3.2.3. Use Two Fingers to Lift Patient's Head past Neutral Position	L R -	✓ ✓ ✓	L R -	L R -	- - -	✓ ✓ ✓
3.3A Place oral airway (Oropharyngeal)		3.3A.1 Apply lubricant 3.3A.2 Place thumb on bottom teeth and index finger on upper teeth 3.3A.3 Move fingers outward to open mouth 3.3A.4 Insert airway upside down until it reaches back of tongue 3.3A.5 Rotate wrist 180 degrees	L/R - - L/R L/R	✓ ✓ ✓ ✓ ✓	L/R - - L/R L/R	L/R - - L/R L/R	- - - - -	✓ ✓ ✓ ✓ ✓
3.3B Place oral airway (Supraglottic)		3.3B.1 Apply lubricant 3.3B.2 Place thumb on bottom teeth and index finger on upper teeth 3.3B.3 Move fingers outward to open mouth 3.3B.4 Hold tube like a pen, place tip against of patients upper teeth 3.3B.5 Insert tube until fully submerged	L/R - - - L/R	✓ ✓ ✓ ✓ ✓	L/R - - - L/R	L/R - - - L/R	- - - - -	✓ ✓ ✓ ✓ ✓

Table A.4.: Hierarchical Task Analysis: Placing an IV Tourniquet

Task	Sub-Sub-Tasks (If Applicable)	Task Movements	Devices					Wearable
			Apple Watch	MYO	Empatic E4	Garmin Watch Forerunner	Bioharness BT	
4. Place an IV Tourniquet								
4.1. Grab Tourniquet Multi-hand Task		4.1.1. Move hand to tourniquet 4.1.2. Close hand to grab tourniquet 4.1.3. Move hand to patient's extremity 4.1.4. Use both hands to place tourniquet under patient's extremity	L/R - L/R L/R	✓ ✓ ✓ ✓	L/R - L/R L/R	L/R - L/R L/R	- - - -	✓ ✓ ✓ ✓
4.2. Tie Tourniquet Multi-Hand Task		4.2.1. Use both hands to cross tourniquet around patient's arm 4.2.2. Tuck one end under the strap so that both ends come out on the same side 4.2.3. Open both hands	L/R R -	✓ ✓ ✓	L/R R -	L/R R -	- - -	✓ ✓ ✓

Table A.5.: Hierarchical Task Analysis: Wrapping a wound

Task	Sub-Sub-Tasks(If Applicable)	Task Movements	Devices					
			Apple Watch	MYO	Empatic E4	Garmin Watch Forerunner	Bioharness BT	Sensed?
5. Wrapping a wound								
5.1. Grab Dressing Multi-Hand Task	5.1.1. Move hand to pressure dressing storage compartment 5.1.2. Close hand to grab pressure dressing 5.1.3. Move hand to patient's wound		L/R - L/R	✓ ✓ ✓	L/R - L/R	L/R - L/R	- - -	✓ ✓ ✓
5.2. Dress Wound Multi-Hand Task	5.2.1. Move hand to pressure dressing storage compartment 5.2.2. Use both hands to wrap pressure dressing around the wound 5.2.3. Tie ends together		L/R L/R L/R	✓ ✓ ✓	L/R L/R L/R	L/R L/R L/R	- - -	✓ ✓ ✓

A.1. Machine Learning Algorithms Parameters

The decision-tree algorithm achieved the highest score using the following parameters:

- `criterion='gini'`
- `splitter='best'`
- `max_depth=None`
- `min_samples_split=2`
- `min_samples_leaf=1`
- `max_leaf_nodes=None`

The SVM algorithm achieved the highest score using the following parameters:

- `kernel='rbf'`
- `C=0.01`
- `gamma=1000`

The k -NN algorithm achieved the highest score using the following parameters:

- `k=4`
- `weights=uniform`
- `algorithm=auto`

The HMM algorithm achieved the highest score using the following parameters:

- `DistributionModel=NormalDistribution`
- `n_components=1`
- `algorithm='baum-welch'`

A.2. 2 Seconds and 4 Seconds Window Sizes

Procedure	decision-tree			k-NN ($k = 4$)			SVM			HMM		
	Precision	Recall	F1	Precision	Recall	F1	Precision	Recall	F1	Precision	Recall	F1
T	0.63	0.64	0.63	0.34	0.56	0.42	0.53	0.66	0.59	0.29	0.39	0.33
W	0.73	0.73	0.73	0.42	0.47	0.44	0.58	0.68	0.63	0.22	0.19	0.20
B	0.20	0.21	0.21	0.15	0.05	0.07	0.18	0.11	0.14	0.70	0.71	0.71
O	0.32	0.32	0.32	0.23	0.05	0.09	0.28	0.17	0.22	0.64	0.44	0.53
C	0.59	0.59	0.59	0.45	0.29	0.36	0.46	0.34	0.39	0.38	0.47	0.42
All	0.60	0.60	0.60	0.38	0.39	0.36	0.49	0.51	0.49	0.48	0.46	0.47

Table A.6.: 2 seconds. Note: T is intravenous tourniquet, W is wrapping a wound, B is Bag-Valve-Mask ventilation, O is oral airway, and C is CPR

Procedure	decision-tree			k-NN ($k = 4$)			SVM			HMM		
	Precision	Recall	F1	Precision	Recall	F1	Precision	Recall	F1	Precision	Recall	F1
T	0.68	0.69	0.69	0.33	0.57	0.41	0.55	0.64	0.59	0.29	0.44	0.35
W	0.77	0.78	0.78	0.40	0.43	0.42	0.57	0.69	0.63	0.29	0.25	0.27
B	0.29	0.28	0.28	0.17	0.04	0.07	0.18	0.10	0.13	0.66	0.67	0.66
O	0.41	0.40	0.41	0.22	0.07	0.10	0.28	0.15	0.20	0.60	0.37	0.46
C	0.65	0.63	0.64	0.37	0.23	0.28	0.46	0.37	0.41	0.32	0.37	0.34
All	0.66	0.66	0.66	0.35	0.36	0.33	0.49	0.52	0.50	0.46	0.44	0.44

Table A.7.: 4 seconds